

Unusual ordered phases of highly frustrated magnets: a review

Oleg A. Starykh¹

¹Department of Physics and Astronomy, University of Utah, Salt Lake City, UT 84112-0830

(Dated: December 29, 2014)

We review ground states and excitations of a quantum antiferromagnet on triangular and other frustrated lattices. We pay special attention to the combined effects of magnetic field h , spatial anisotropy R , and spin magnitude S . The focus of the review is on the novel collinear spin density wave and spin nematic states, which are characterized by *fully gapped* transverse spin excitations with $S^z = \pm 1$. We discuss extensively $R - h$ phase diagram of the antiferromagnet, both in the large- S semiclassical limit and the quantum $S = 1/2$ limit. When possible, we point out connections with experimental findings.

[This is the originally submitted version of the invited review, to be published in Reports on Progress in Physics in 2015. The link, via DOI, to the accepted and published version of the manuscript, which is updated according to the referees comments, will be provided upon its actual publication.]

Contents

I. Introduction	1
II. Classical model in a magnetic field	2
III. Quantum model in magnetic field	4
A. Isotropic triangular lattice	4
B. Spatially anisotropic triangular antiferromagnet with $J' \neq J$	5
C. Spin 1/2 spatially anisotropic triangular antiferromagnet with $J' \neq J$	8
IV. SDW and nematic phases of spin-1/2 models	9
A. SDW	9
1. SDW in a system of Ising-like coupled chains	10
2. Magnetization plateau as a commensurate collinear SDW phase	11
B. Spin nematic	11
1. Weakly coupled nematic chains	11
2. Spin-current nematic state at the 1/3-magnetization plateau	12
C. Magnetization plateaus in itinerant electron systems	12
V. Experiments	13
A. Magnetization plateau	14
B. SDW and spin nematic phases	15
C. Weak Mott insulators: Hubbard model on anisotropic triangular lattice	15
Acknowledgments	16
References	16

I. INTRODUCTION

Frustrated quantum antiferromagnets have been at the center of intense experimental and theoretical investigations for many years. These relentless efforts have very recently resulted in a number of theoretical and experimental breakthroughs: quantum entanglement¹⁻³, density matrix renormal-

ization group (DMRG) revolution and Z_2 liquids in kagomé and $J_1 - J_2$ square lattice models⁴⁻⁶, spin-liquid-like behavior in organic Mott insulators^{7,8} and kagomé lattice antiferromagnet herbertsmithite⁹.

Along the way, a large number of frustrated insulating magnetic materials featuring rather unusual *ordered* phases, such as magnetization plateaux, longitudinal spin-density waves, and spin nematics, has been discovered and studied. It is these ordered, yet sufficiently unconventional, states of magnetic matter and theoretical models motivated by them that are the subject of this Key Issue article.

This review focuses on materials and models based on simple triangular lattice, which, despite many years of fruitful research, continue to supply us with novel quantum states and phenomena. Triangular lattice represents, perhaps, the most widely studied frustrated geometry¹⁰⁻¹². Indeed, the Ising antiferromagnet on the triangular lattice was the first spin model found to possess a disordered ground state and extensive residual entropy¹³ at zero temperature. While the classical Heisenberg model on the triangular lattice does order at $T = 0$ into a well-known 120° commensurate spiral pattern (also known as a three-sublattice or $\sqrt{3} \times \sqrt{3}$ state), the fate of the quantum spin-1/2 Heisenberg Hamiltonian has been the subject of a long and fruitful debate spanning over 30 years of research. Eventually it was firmly established that the quantum spin-1/2 model remains ordered in the classical 120° pattern¹⁴⁻¹⁶. Although the originally proposed resonating valence bond liquid^{17,18} did not emerge as the ground state of the spin-1/2 Heisenberg model, such a phase was later found in a related quantum dimer model on the triangular lattice.¹⁹

It turns out that a simple generalization of the triangular lattice Heisenberg model whereby exchange interactions on the nearest-neighbor bonds of the triangular lattice take two different values – J on the horizontal bonds and J' on the diagonal bonds, as shown in Figure 1 – leads to a very rich and not yet fully understood phase diagram which sensitively depends on the magnitude of the site spin S and magnetic field h . Such a distorted, or spatially anisotropic, triangular lattice model interpolates between simple unfrustrated square lattice ($J = 0, J' \neq 0$), strongly frustrated triangular lattice ($J = J' \neq 0$) and decoupled spin chains ($J \neq 0, J' = 0$).

An unexpectedly large number of experimental systems

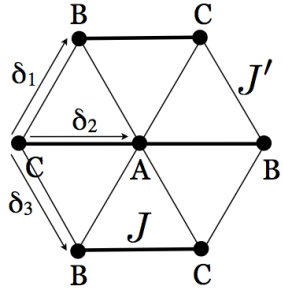


FIG. 1: Deformed triangular lattice. Solid (thin) lines denote bonds with exchange constant J (J') correspondingly. Also indicated are nearest-neighbor vectors δ_j as well as A, B and C sublattice structure.

seems to fit into this simple distorted triangular lattice model with spin $S = 1/2$: Cs_2CuCl_4 (shows extended spinon continuum, $J'/J = 0.34$), Cs_2CuBr_4 (shows magnetization plateau, $J'/J \approx 0.7$) and $\text{Ba}_3\text{CoSb}_2\text{O}_9$ (shows magnetization plateau, $J'/J \approx 1$). Importantly, a number of very interesting organic Mott insulators of $\text{X}[\text{Pd}(\text{dmit})_2]_2$ and $\kappa\text{-(ET)}_2\text{Z}$ families can also be approximately described by the spatially anisotropic $J - J'$ model with additional ring-exchange (involving four spins and higher order) terms. It is widely believed that these materials are weak Mott insulators in a sense of being close to a metal-insulator transition. As such, they are best described by distorted $t - t' - U$ Hubbard model, so that spatial anisotropy of exchanges follows from that of single particle hopping parameters, $J'/J \sim (t'/t)^2$.

The (intentionally) rather narrow focus of the review leaves out several important recent developments. Kagomé lattice antiferromagnets represent perhaps the most notable omission. A lot is happening there, both in terms of experiments on materials such as herbertsmithite and volborthite²⁰ and in terms of theoretical developments^{4,9}. This very important area of frustrated magnetism deserves its own review. We also have avoided another very significant area of development – systems with significant spin-orbit interactions. Progress in this area has been summarized in recent reviews^{21,22}.

The presentation is organized as follows: Section II contains brief review of the states of classical model in a magnetic field. Section III describes phase diagrams of the semiclassical $S \gg 1$ (Section III B) and $S = 1/2$ (Section III C) models. Novel ordered states, a collinear SDW and a spin nematic, which are characterized by the absence of $S = 1$ transverse spin excitations, are described in Section IV. Section V summarizes key experimental findings relevant to the review, including recent developments in organic Mott insulators.

II. CLASSICAL MODEL IN A MAGNETIC FIELD

Triangular antiferromagnets in an external magnetic field have been extensively studied for decades, and found to possess unusual magnetization physics that remains only partially understood. Underlying much of this interesting behavior is the discovery, made long ago,²³ that in a magnetic field,

Heisenberg spins with isotropic exchange interactions exhibit a large *accidental* classical ground-state degeneracy. That is, at finite magnetic fields, there exists an infinite number of continuously deformable classical spin configurations that constitute minimum energy states, but are *not* symmetry related.

This degeneracy is understood by the observation that the Hamiltonian of the isotropic triangular lattice antiferromagnet in magnetic field \mathbf{h} can be written, up to an unessential constant, as

$$H_0 = \frac{J}{2} \sum_{\mathbf{r}} \left[\mathbf{S}_{\mathbf{r}} + \mathbf{S}_{\mathbf{r}+\delta_1} + \mathbf{S}_{\mathbf{r}+\delta_2} - \frac{\mathbf{h}}{3J} \right]^2. \quad (1)$$

The sum is over all sites \mathbf{r} of the lattice and nearest-neighbor vectors $\delta_{1,2}$ are indicated in the Figure 1. Note that Zeeman terms $\mathbf{S}_{\mathbf{r}} \cdot \mathbf{h}$ appear three times for every spin in this sum, which explains the factor of $1/3$ in the \mathbf{h} term in (1). We immediately observe that every spin configuration which nullifies every term in the sum (1) belongs to the lowest energy manifold of the model. Given the *side-sharing* property of the triangular lattice, so that fixing all spins in one elementary triangle fixes two spins in each of the adjacent triangles, sharing sides with the first one, this implies that all such states exhibit a three-sublattice structure and must satisfy

$$\mathbf{S}_A + \mathbf{S}_B + \mathbf{S}_C = \frac{\mathbf{h}}{3J}. \quad (2)$$

This condition provides 3 equations for 6 angles needed to describe 3 classical unit vectors. In the absence of the field, the 3 undetermined angles can be thought of as Euler's angles of the plane in which the spins spontaneously form a three-sublattice 120° structure. However, this remarkable feature persists for $\mathbf{h} \neq 0$ as well. There, the symmetry of the Hamiltonian (1) is reduced to $U(1)$ but the degeneracy persists: one of the free angles can be thought as gauge degree of freedom to rotate all spins about the axis of the field \mathbf{h} , while the remaining two constitute the phenomenon of *accidental degeneracy*.

Remarkably, thermal (entropic) fluctuations lift this extensive degeneracy in favor of the two *coplanar* (Y and V states) and one *collinear* (UUD) spin configurations, shown in Figure 2. Symmetry-wise, coplanar states break two different symmetries – a discrete Z_3 symmetry, which corresponds to the choice of sublattice on which the down spin (in the case of Y) or the minority spin (in the case of V) is located, and a continuous $U(1) = O(2)$ symmetry of rotations about the field axis. The collinear UUD state breaks only the discrete Z_3 symmetry (a choice of sublattice for the down spin). Selection of these simple states out of infinitely many configurations, which satisfy (2), by thermal fluctuations represents a textbook example of the ‘order-by-disorder’ phenomenon²⁴.

The resulting enigmatic phase diagram, first sketched by Kawamura and Miyashita in 1985, Ref. 23, continues to attract much attention - and in fact remains not fully understood. Figure 3 shows the result of recent simulations²⁵, which studied critical properties of various phase transitions in great detail, differs in important aspect from the original suggestion –

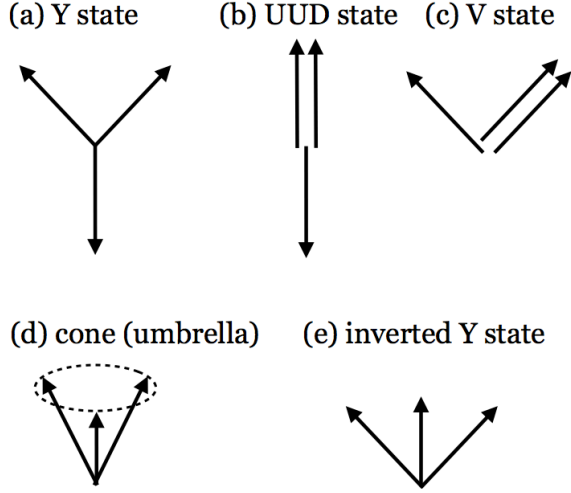


FIG. 2: Various spin configurations from the classical ground state manifold. (a) coplanar Y state, (b) collinear UUD (up-up-down), (c) coplanar V state, (d) non-coplanar cone (umbrella) state, (e) inverted Y state.

it is established now that there is no direct transition between the Y state and the paramagnetic phase (very similar results were obtained in an extensive study²⁶). The two phases are separated by the intervening UUD state which extends down to lowest accessible field values and before the transition to the paramagnetic state. Figure 3 also shows that of all entropically selected state, the UUD state is most stable - it extends to higher T than either Y or V states.

The UUD is also the most ‘visible’ of the three selected states - it shows up as a plateau-like feature in the magnetization curve $M(h)$, see Figure 4 which shows experimental data for a $S = 5/2$ triangular lattice antiferromagnet $\text{RbFe}(\text{MoO}_4)_2$ ²⁷. Notice that a strict magnetization plateau at $1/3$ of the full (saturation) value M_{sat} , $M = M_{\text{sat}}/3$, is possible only in the quantum problem (*i.e.* the problem with finite spin S), when all spin-changing excitations with $S^z \neq 0$ are characterized by *gapped* spectra, and at absolute zero $T = 0$, when no excitations are present in the ground state (see next Section III for complete discussion). At any finite T thermally excited spin waves are present and lead to a finite, albeit different from the neighboring non-plateau states, slope of the magnetization $M(h)$. In the case of the classical problem we review here the gap in spin excitation spectra is itself T -dependent and disappears as $T \rightarrow 0$: as a result its magnetization ‘quasi-plateau’ too disappears in the $T \rightarrow 0$ limit. However, at any finite T , less than that of the transition to the paramagnetic state, the slope of the $M(h)$ for the UUD state is different from that of the Y and V states²⁸.

The most outstanding, and still not resolved issue, is the conjectured $SO(3)$ breaking transition²⁹ at $T_v \approx 0.285J$ and $h = 0$. The transition is driven by the proliferation, above the critical temperature T_v , of the Z_2 vortices, which are defects of spin chirality²⁹. It is by now established that unlike the case of Berezinsky-Kosterlitz-Thouless vortex-unbinding transition³⁰, the spin correlation length remains finite (albeit

very large) below T_v , resulting in a disordered ‘spin-gel’ state³¹. Whether the change from high-temperature vortex-dominated regime to the low-temperature spin-fluctuation-dominated one is a true transition or a sharp crossover remains the topic of active debate^{32–36}. Experimental ramifications of this interesting scenario are reviewed in³⁷.

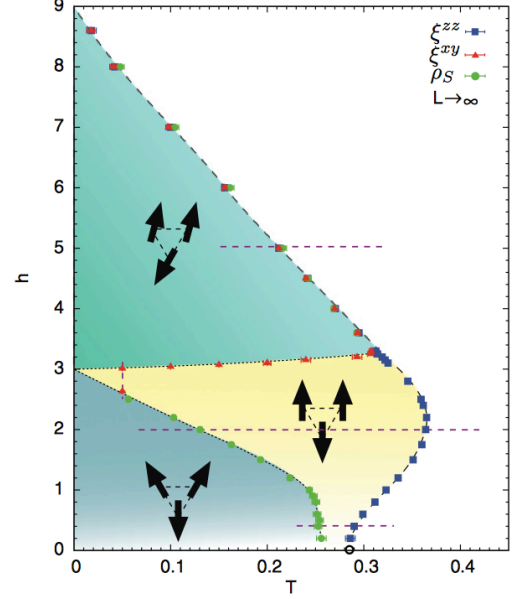


FIG. 3: Magnetic field phase diagram of the classical triangular lattice antiferromagnet. [Adapted from Seabra *et al.*, Phys. Rev. B **84**, 214418 (2011). Copyright 2011 by the American Physical Society.] Transition points determined by the Monte Carlo simulations are shown by filled symbols. Continuous phase transitions are drawn with a dashed line, while Berezinskii-Kosterlitz-Thouless phase transitions are drawn with a dotted line. For fields $h \leq 3$ a double transition is found upon cooling from the paramagnet, while for $h \geq 3$ only a single transition is found. Behavior of the phase transition lines in the low-field region $h \leq 0.2$, which is left unshaded in the diagram, is not settled at the present. See Ref.31 for the recent study of $h = 0$ line.

A classical system with spatially anisotropic interactions offers an interesting generalization of the ‘order-by-disorder’ phenomenon. Consider slightly deformed triangular lattice, with $J' < J$ (see Fig. 1). An arbitrary weak deformation lifts, at $T = 0$, the accidental degeneracy in favor of the simple non-coplanar umbrella state (configuration ‘d’ in Fig. 2) in the whole range of h below the saturation field. The energy gain of this well-known spin configuration is of the order $(J - J')^2/J$. One thus can expect that, for sufficiently small difference $R = J - J'$, entropic fluctuations, which favor coplanar and collinear spin states at a finite T , can still overcome this classical energy gain and stabilize collinear and coplanar states *above* some critical temperature which can be estimated as $T_{\text{umb-uud}} \sim R^2/J$. As a result, the UUD phase ‘decouples’ from the $T = 0$ axis. The leftmost point of the UUD phase in the $h - T$ phase diagram now occurs at a finite $T_{\text{umb-uud}}$ as was indeed observed in Monte Carlo simulation of the simple triangular lattice model in Ref.28 (see Fig.10

of that reference), as well as in a more complicated ones, for models defined on deformed pyrochlore³⁸ and Shastry-Sutherland³⁹ lattices. It is worth noting that the roots of this behavior can be traced to the famous Pomeranchuk effect in ³He, where the crystal phase has higher entropy than the normal Fermi-liquid phase. As a result, upon heating, the liquid phase *freezes* into a solid^{40,41}. In the present classical spin problem it is ‘superfluid’ umbrella phase which freezes into a ‘solid’ UUD phase upon heating (see discussion of the relevant terminology at the end of Section III A below).

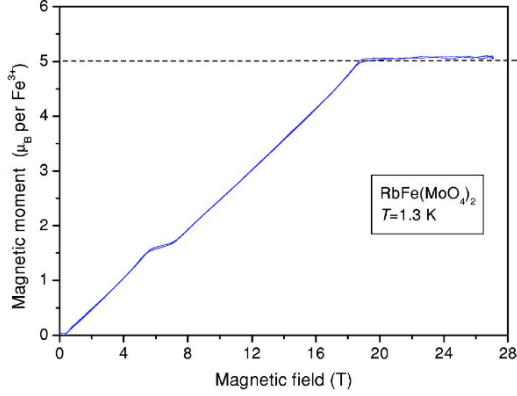


FIG. 4: Magnetization curve $M(h)$ of a spin-5/2 antiferromagnet $\text{RbFe}(\text{MoO}_4)_2$ at $T = 1.3\text{K}$. [Adapted from Smirnov *et al.*, Phys. Rev. B **75**, 134412 (2007). Copyright 2007 by the American Physical Society.]

III. QUANTUM MODEL IN MAGNETIC FIELD

A. Isotropic triangular lattice

Much of the intuition about selection of coplanar and collinear spin states by thermal fluctuations applies to the most interesting case of *quantum* spin model on a (deformed) triangular lattice. Only now it is quantum fluctuations (zero-point motion) which differentiate between different classically-degenerate (or, nearly degenerate) states and lift the accidental degeneracy.

One of the first explicit calculations of this effect was carried out by Chubukov and Golosov⁴², who used semiclassical large- S spin wave expansion in order to systematically separate classical and quantum effects. This well-known technique relies on Holstein-Primakoff representation of spin operators in terms of bosons. The representation is nonlinear, $S_{\mathbf{r}}^z = S - a_{\mathbf{r}}^\dagger a_{\mathbf{r}}$, $S_{\mathbf{r}}^+ = (2S - a_{\mathbf{r}}^\dagger a_{\mathbf{r}})^{1/2} a_{\mathbf{r}}$, and leads, upon expansion of square roots in powers of small parameter $1/S$, to bosonic spin-wave Hamiltonian $H = E_{\text{cl}} + \sum_{k=2}^{\infty} H^{(k)}$. Here E_{cl} stands for the classical energy of spin configuration, which scales as S^2 , while each of the subsequent terms $H^{(k)}$ are of k -th order in operators $a_{\mathbf{r}}$ and scale as $S^{2-k/2}$. Diagonalization of quadratic term $H^{(2)}$ provides one with the dispersion $\omega_{\mathbf{k}}^{(m)}$ of spin wave excitations (\mathbf{k} is the wave vector and m is the band index), in terms of which quantum zero-point energy

is given by $\langle H^{(2)} \rangle = (1/2) \sum_{m,\mathbf{k}} \omega_{\mathbf{k}}^{(m)}$. This energy scales as S , and thus provides the leading quantum correction to the classical ($\propto S^2$) result.

The main outcome of the calculation⁴² is the finding that quantum fluctuations too selects coplanar Y and V and collinear UUD states (states a, b and c in Figure 2) out of many other classically degenerate ones. The authors also recognized the key special feature of the UUD state - being collinear, this state preserves $U(1)$ symmetry of rotations about the magnetic field axis. The absence of broken continuous symmetry implies that spin excitations have a finite energy gap in the dispersion. This expectation is fully confirmed by the explicit calculation⁴² which finds that the gaps of the two low energy modes are given by $|h - h_{c1,c2}^0|$, where the lower/upper critical fields are given by $h_{c1}^0 = 3JS - 0.5JS/(2S)$ and $h_{c2}^0 = 3JS + 1.3JS/(2S)$, correspondingly. (The third mode describes a high-energy precession with energy hS .) The uniform magnetization M , being the integral of motion, remains at $1/3$ of the maximum (saturation) value, $M = M_{\text{sat}}/3$, in the UUD stability interval $h_{c1}^0 < h < h_{c2}^0$.

As a result, magnetization curve $M(h)$ of the quantum triangular lattice antiferromagnet is non-monotonic and exhibit striking $1/3$ magnetization plateau in the finite field interval $\Delta h = h_{c2}^0 - h_{c1}^0 = 1.8JS/(2S)$. It is worth noting that this is not a narrow interval at all, $\Delta h/h_{\text{sat}} = 0.2/(2S)$ in terms of the saturation field $h_{\text{sat}} = 9JS$. Extending this large- S result all way to the $S = 1/2$ implies that the magnetization plateau takes up 20% of the whole magnetic field interval $0 < h < h_{\text{sat}}$.

Numerical studies of the plateau focus mostly on the quantum spin-1/2 problem (numerical studies of higher spins are much more ‘expensive’) and confirm the scenario outlined above. The plateau at $M = M_{\text{sat}}/3$ is indeed found, and moreover its width in magnetic field agrees very well with the described above large- S result, extrapolated to $S = 1/2$.^{43–48}

The pattern of symmetry breaking by the coplanar/collinear states is described by the following spin expectation values

$$\begin{aligned} \text{Y state, } 0 < h < h_{c1}^0 : \langle S_{\mathbf{r}}^+ \rangle &= ae^{i\varphi} \sin[\mathbf{Q} \cdot \mathbf{r}], \\ \langle S_{\mathbf{r}}^z \rangle &= b - c \cos^2[\mathbf{Q} \cdot \mathbf{r}]; \end{aligned} \quad (3)$$

$$\begin{aligned} \text{UUD state, } h_{c1}^0 < h < h_{c2}^0 : \langle S_{\mathbf{r}}^+ \rangle &= 0, \\ \langle S_{\mathbf{r}}^z \rangle &= M - c \cos[\mathbf{Q} \cdot \mathbf{r}]; \end{aligned} \quad (4)$$

$$\begin{aligned} \text{V state, } h_{c1}^0 < h < h_{\text{sat}} : \langle S_{\mathbf{r}}^+ \rangle &= ae^{i\varphi} \cos[\mathbf{Q} \cdot \mathbf{r}], \\ \langle S_{\mathbf{r}}^z \rangle &= b - c \cos^2[\mathbf{Q} \cdot \mathbf{r}]. \end{aligned} \quad (5)$$

Here the ordering wave vector $\mathbf{Q} = (4\pi/3, 0)$ is commensurate with the lattice which results in only three possible values that the product $\mathbf{Q} \cdot \mathbf{r} = 2\pi\nu/3$ can take ($\nu = 0, 1, 2$), modulo 2π . Angle φ specifies orientation of the ordering plane for coplanar spin configurations within the $x - y$ plane, M is magnetization per site, and parameters a, b, c are constants dependent upon the field magnitude.

Connection with ‘super’ phases of bosons: Eq.(4) identifies UUD state as a collinear ordered state which can be thought of as *solid*. Its ‘density’ $\langle S_{\mathbf{r}}^z \rangle$ is *modulated* as $\cos[\mathbf{Q} \cdot \mathbf{r}]$, as appropriate for the solid, and as a result its local magnetization follows simple ‘up-up-down’ pattern within each

elementary triangle. It obviously respects $U(1)$ symmetry of rotations about S^z axis. The coplanar Y and V states break this $U(1)$ symmetry by spontaneously selecting angle φ . Note that in addition they are characterized by the modulated density $\langle S_r^z \rangle$, which makes them *supersolids*: the superfluid order (magnetic order in the $x-y$ plane as selected by φ) co-exists with the solid one (modulated z component, or density). This useful connection is easiest to make precise⁴⁹ in the case of $S = 1/2$ when the following mapping between a *hard-core* lattice Bose gas and a spin-1/2 quantum magnet can easily be established:

$$a_r^+ \leftrightarrow S_r^+, a_r \leftrightarrow S_r^-, n_r = a_r^+ a_r \leftrightarrow S_r^z - 1/2. \quad (6)$$

The superfluid order is associated with finite $\langle a_r^+ \rangle$ while the solid one with modulated (with momentum \mathbf{Q} in our notations) boson density $\langle n_r \rangle$.

B. Spatially anisotropic triangular antiferromagnet with $J' \neq J$

Consider now a simple deformation of the triangular lattice which makes exchange interaction on diagonal bonds, J' , different from those on horizontal ones J , so that $R = J - J' \neq 0$. This simple generalization of the Heisenberg model leads to surprisingly complicated and not yet fully understood phase diagram in the magnetic field (h) - deformation (R) plane.

Semiclassical ($S \gg 1$) analysis of this problem is complicated by the fact that arbitrary small $R \neq 0$ removes accidental degeneracy of the problem in favor of the unique non-coplanar and incommensurate cone (umbrella) state, already discussed in Sec. II, state ‘d’ in Fig. 2. This simple state gains energy of the order $\delta E_{\text{class}} \sim S^2 R^2 / J$ per spin. Its structure is described by

$$\langle \mathbf{S}_r \rangle = M \hat{z} + c(\cos[\mathbf{Q}' \cdot \mathbf{r} + \varphi] \hat{x} + \sin[\mathbf{Q}' \cdot \mathbf{r} + \varphi] \hat{y}), \quad (7)$$

where classically the ordering wave vector $\mathbf{Q}' = (2 \cos^{-1}[-J'/2J], 0)$ is a continuous function of J'/J . Being non-coplanar, this state is characterized by the finite chirality $\chi \sim \mathbf{S}_r \cdot \mathbf{S}_{r+\delta_1} \times \mathbf{S}_{r+\delta_2} \sim M(2 \sin[\mathbf{Q}' \cdot \delta_1] - \sin[\mathbf{Q}' \cdot \delta_2])$.

At the same time, for sufficiently small R , the quantum energy gain due to zero-point motion of spins, which is of the order $\delta E_q \sim SJ$ per spin, should be able to overcome δE_{class} and still stabilize one of the coplanar/collinear states considered in Sec. III A above. Comparing the two contributions, we conclude, following Ref. 50, that the classical-quantum competition can be parameterized by the dimensionless parameter $\delta \sim \delta E_{\text{class}} / \delta E_q \sim S(R/J)^2$. (In the following, we will use more precise value $\delta = (40/3)S(R/J)^2$, with numerical factor 40/3 as introduced in⁵⁰ for technical convenience.)

Explicit consideration of this competition is rather difficult due to complicated dependence of the parameters of the coplanar states on magnetic field h and exchange deformation R . However, inside the $M = M_{\text{sat}}/3$ magnetization plateau phase, the spin structure is actually pretty simple, as equation (4) shows, which suggests that UUD state can be

used as a convenient starting point for accessing more complicated states. This approach, which amounts to the investigation of the *local stability* of the UUD phase, was carried out in⁵⁰. Similar to⁴², the calculation is based on the three-spin UUD unit cell, resulting in three spin wave branches. One of these, describing total spin precession, is a high-energy mode not essential for our analysis, while the two others, which describe relative fluctuations of spins, are the relevant low-energy modes.

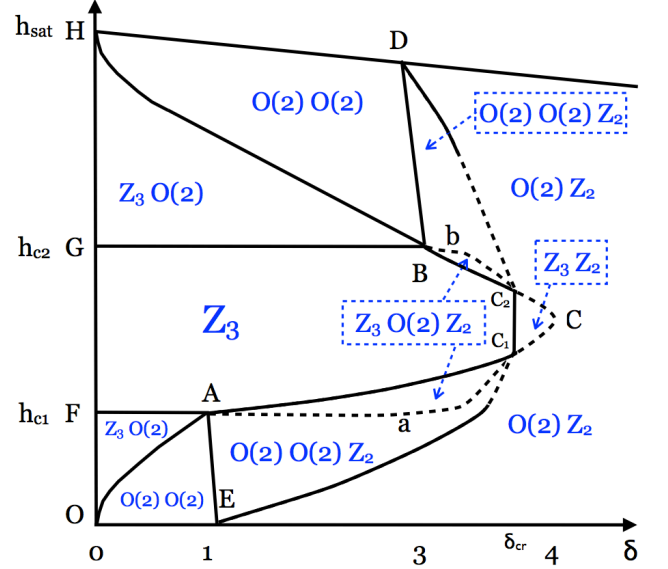


FIG. 5: Schematic large- S phase diagram of the deformed triangular lattice antiferromagnet. Phase boundary lines are schematic and serve to indicate possible shape only approximately. Dashed lines indicate location of conjectured phase transitions. Capital letters A through O indicated various (multi)critical points discussed in the text. Each phase is characterized by the set of broken symmetries, as indicated by (blue) symbols. Observe that the line H-B-b-C₂-C-C₁-a-A-O is the transition line separating phases with broken Z_3 from those with broken $O(2)$. This phase diagram is based on Refs. 50–52.

Within the UUD plateau phase, which is bounded by FACBG lines in Figure 5, both low energy spin wave modes remain gapped. As discussed above, the only symmetry this collinear state breaks is Z_3 . The gaps of the low-energy spin wave modes (to be called mode 1 and mode 2 in the following) are given by $|h - h_{c1,c2}|$, where now the lower and upper critical fields $h_{c1,c2}(\delta)$ depend on the dimensionless deformation parameter δ . Gap’s closing at the lower h_{c1} (upper h_{c2}) critical fields of the plateau implies Bose-Einstein condensation (BEC) of the appropriate magnon mode (1 or 2) and the appearance of the transverse to the field spin component $\langle S_r^+ \rangle \neq 0$, see (3) and (5). This BEC transition breaks spin rotational $U(1)$ symmetry via spontaneous selection of the ‘superfluid’ phase φ . The spin structure of the resulting ‘condensed’ state sensitively depends on the wave vector $\mathbf{k}_{1/2}$ of the condensed magnon.

Key results of the large- S calculation in Refs. 50–52 can now be summarized as follows:

(a) In the interval $0 < \delta \leq 1$ the lower critical field is actually

independent of δ , $h_{c1} = h_{c1}^0$, and the minimum of the spin wave mode 1 remains at $\mathbf{k}_1 = 0$. As a result, BEC condensation of mode 1 at $h = h_{c1}$ signals the transition to the commensurate Y state, which lives in the region OAF in Figure 5. In addition to breaking the continuous $U(1)$ symmetry, the Y state inherits broken Z_3 from the UUD phase (which corresponds to the selection of the sublattice for the *down* spins).

(b) For $1 < \delta \leq 4$, the low critical field increases and, simultaneously, the spin wave minima shift from zero to finite momenta $\pm \mathbf{k}_1 = (\pm k_1, 0)$. Thus, at $h = h_{c1}$, the spectrum softens at two different wave vectors at the same time. This opens an interesting possibility of the simultaneous coherent condensation of magnons with opposite momenta $+\mathbf{k}_1$ and $-\mathbf{k}_1$.⁵³ It turns out, however, that repulsive interaction between condensate densities at $\pm \mathbf{k}_1$ makes this energetically unfavorable⁵⁰. Instead, at the transition the symmetry between the two possible condensates is broken spontaneously and magnons condense at a single momentum, $+\mathbf{k}_1$ or $-\mathbf{k}_1$. The resulting state, denoted as *distorted umbrella* in⁵⁰, is characterized by the broken Z_3 , $U(1)$ and Z_2 symmetries – the latter corresponds to the choice $+\mathbf{k}_1$ or $-\mathbf{k}_1$. This non-coplanar state lives in the narrow region bounded by lines AC_1 (solid) and AaC_1 (dashed) in Figure 5.

(c) Similar developments occur near the upper critical field h_{c2} . In the interval $0 < \delta \leq 3$ the upper critical field is actually independent of δ , $h_{c2} = h_{c2}^0$, and the minimum of the spin wave mode 2 remains at $\mathbf{k}_2 = 0$. The transition on the line GB is towards the coplanar and commensurate V state, bounded by GBH in Figure 5. This state is characterized by broken $Z_3 \times U(1)$ symmetries.

(d) In the interval $3 < \delta \leq 4$, the upper field h_{c2} diminishes and simultaneously the minimum of the mode 2 shifts from zero momentum to the two degenerate locations at $\pm \mathbf{k}_2 = (\pm k_2, 0)$. Here, too, at the condensation transition (along the line BC_2) it is energetically preferable to break Z_2 symmetry between the two condensates and to spontaneously select just one momentum, $+\mathbf{k}_2$ or $-\mathbf{k}_2$. This leads to *distorted umbrella* with broken $Z_3 \times U(1) \times Z_2$ symmetries. This state lives between (solid) BC_2 and (dashed) BbC_2 lines in Figure 5.

(e) *Spin nematic region*. The critical fields h_{c1} and h_{c2} merge at the plateau's end-point $\delta = 4$ (point C). The minima of the spin wave modes 1 and 2 coincide at this point $\mathbf{k}_1 = \mathbf{k}_2 = (k_0, 0)$ with $k_0 = \sqrt{3}/(10S)$. The end-point of the UUD phase thus emerges as a point of an extended symmetry hosting four linearly-dispersing gapless spin wave modes⁵⁰ (two branches, each gapless at $(\pm k_0, 0)$). Single-particle analysis of possible instabilities at the plateau's end-point (point C, $\delta = 4$) shows that in addition to the expected $U(1) \times U(1)$ symmetry (the two $U(1)$'s represent phases of the single particle condensates), the state at $\delta = 4$ point poses an unusual P_1 symmetry – the magnitude of the condensate at this point is not constrained⁵⁰. The enhanced degeneracy of the plateau's end point C can also be understood from the observation that the two chiral distorted umbrella states merging at the point C are characterized, quite generally, by the *different* chiralities: Condensation of magnons at $h_{c1,c2}$, described in items (b) and (c) above, proceed independently of each other – hence the

chiralities of the two states are not related in any way. Thus the merging point of the two phases, point C, must possess enhanced symmetry.

Unconstrained magnitude mode hints at a possibility of a *two-particle condensation* – and indeed recent work⁵¹ has found that a single-particle instability at $\delta = 4$ is pre-empted by the two-particle one at a slightly smaller value of $\delta = \delta_{cr} = 4 - O(1/S^2)$. This is indicated by the (dashed) line C_1 - C_2 in the Figure. This happens via the development of the ‘superconducting’-like instability of the magnon pair fields $\Psi_{1,p} = d_{1,+k_0+p}d_{2,-k_0-p}$ and $\Psi_{2,p} = d_{1,-k_0+p}d_{2,+k_0-p}$ and consists in the appearance of two-particle condensates $\langle \Psi_{1,p} \rangle = \langle \Psi_{2,p} \rangle = i\Upsilon/|p|$. The sign of the real-valued Ising order parameter Υ determines the sense of spin-current circulation on the links of the triangular lattice, as illustrated in Figure 6. The spin current is defined as the ground state expectation value of the vector product of neighboring spins. For example, spin current on the AC link of the elementary triangle is given by $\mathcal{J}_{AC}^z = \hat{z} \cdot \langle \mathbf{S}_A \times \mathbf{S}_C \rangle \sim \Upsilon$. In addition to spin currents, this novel state also supports finite spin chirality, $\langle \mathbf{S}_A \cdot \mathbf{S}_B \times \mathbf{S} \rangle \sim \Upsilon$, even though $\langle S_{A/B/C}^{x,y} \rangle = 0$ for each of the spins individually. At the same time, in the absence of single-particle condensation, $\langle d_{1/2} \rangle = 0$, the usual two-point spin correlation function $\langle S^a(\mathbf{r}) S^b(0) \rangle$ is not affected by the two-particle $\langle \Psi_{1/2} \rangle \neq 0$ condensate: its transverse ($a = b = x$ or y) components continue to decay exponentially because of the finite energy gap in the single magnon spectra, while the longitudinal ($a = b = z$) components continue to show a perfect UUD crystal order.

Hence the resulting state, which lives inside triangle-shaped region C_1 - C - C_2 in Figure 5, is a *spin-nematic* state. It can also be called a *spin-current* state⁵¹. It is uniquely characterized by the sign of Υ which determines the sense (clockwise or counterclockwise) of spin current circulation. The spin-current nematic is an Ising-like phase with massive excitations, which are domain walls separating domains of oppositely circling spin currents. It is characterized by broken $Z_3 \times Z_2$, where Z_2 is the sign of the two-magnon order parameter Υ in the ground state. It is useful to note that spontaneous selection of the circulation direction can also be viewed as a spontaneous breaking of the spatial inversion symmetry $\mathcal{I} : x \rightarrow -x$, which changes direction of spin currents on all bonds. (A different kind of nematic is discussed in Section IV B.)

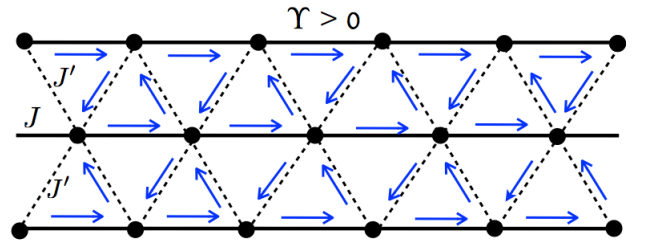


FIG. 6: Pattern of spin currents in the spin nematic phase, for $\Upsilon > 0$.

(f) *high-field region*, $h_{c2}(\delta) \ll h \leq h_{sat}(\delta)$. The high field region, $h \approx h_{sat}(\delta)$, can be conveniently analyzed within powerful Bose-Einstein condensation (BEC) framework. This fol-

lows from the simple observation that the ground state of the spin- S quantum model becomes a simple fully polarized state once the magnetic field is greater than the saturation field, $h > h_{\text{sat}}(\delta)$ (which itself is a function of spin S and exchange deformation R). Excitations above this exact ground state are standard spin waves minimal energy for creating which is given by $h - h_{\text{sat}}$. Similar to the situation near plateau's critical field $h_{c1/c2}$, these spin waves are characterized by non-trivial dispersion with two degenerate minima at momenta $\pm \mathbf{Q}'$ (see expression below (7)).

Spontaneous condensation in one of the minima, which constitutes breaking of Z_2 symmetry, results in the usual *cone*, or *umbrella*, state which is characterized by the spin pattern (7) which breaks spin-rotational $O(2)$. This state is realized to the right of the D-C₂ line in Figure 5.

Instead, simultaneous condensation of the high-field magnons in *both* minima results in the *coplanar* state⁵³ (also known as fan state) of the V type. For any $\delta \neq 0$ the wave vector \mathbf{Q}' is not commensurate with the lattice, which makes the coplanar state to be *incommensurate* as well. The condensates $\Psi_{1,2} = \sqrt{\rho} e^{i\theta_{1,2}}$ at wave vectors $\pm \mathbf{Q}'$ have equal magnitude $\sqrt{\rho}$ and each breaks $U(1)$ symmetry. By choosing the phases $\theta_{1,2}$, the resulting state breaks *two* $O(2)$ symmetries. In total, the coplanar state is characterized by the broken $O(2) \times O(2)$. It is instructive to think of these symmetries in a slightly different way - as of those associated with the total $\theta_+ = \theta_1 + \theta_2$ and the relative $\theta_- = \theta_1 - \theta_2$ phases. The spin structure of this state is described by the incommensurate version of (5) which can be obtained by identifying $\varphi = \theta_+$ and replacing $\cos[\mathbf{Q} \cdot \mathbf{r}] \rightarrow \cos[\mathbf{Q}' \cdot \mathbf{r} + \theta_-]$. The latter replacement shows that the relative $O(2)$ symmetry, associated with the phase θ_- , can also be thought of as a *translational* symmetry associated with the shift of the spin configuration by the vector \mathbf{r}_0 such that $\mathbf{Q}' \cdot \mathbf{r}_0 = \theta_-$, modulo 2π .

Moving to the left, we come to the special *commensurate* point, $\delta = 0$ at $h = h_{\text{sat}}$. Here $\mathbf{Q}' \rightarrow \mathbf{Q} = (4\pi/3, 0)$, resulting in the commensurate coplanar V state. As noted right below Eq. (5), here $\mathbf{Q} \cdot \mathbf{r} = 2\pi\nu/3$, with $\nu = 0, 1, 2$, making the V state a three-sublattice one. Continuous $O(2)$ translational symmetry of the incommensurate V phase is replaced here by the discrete Z_3 symmetry. In other words, the relative phase θ_- is now restricted to the set of three equivalent (up to a global translation of the lattice) degenerate values. The $Z_3 \rightarrow O(2)$ transition across the line H-B between the two coplanar states is thus of a commensurate-incommensurate transition (CI) type. It is described by the classical two-dimensional sine-Gordon model with the nonlinear $\cos[3\theta_-]$ potential describing the locking of the relative phase to the Z_3 set.⁴⁷ In the vicinity of point H in the diagram the line of the CI transition follows $h_{\text{sat}} - h \sim \sqrt{\delta}$.⁵² While the arguments presented here are valid in the immediate vicinity of h_{sat} , the identification of the whole line H-B as the CIT line between the commensurate and incommensurate V states is possible due to the additional evidence reported in item (c) above - commensurate V state is reached from the UUD state in the whole interval $0 < \delta \leq 3$.

The next task is to connect the incommensurate coplanar V state, which occupies region HDB in Figure 5, with the in-

commensurate cone state, to the right of D-C₂ line. Since the V state has equal densities of bosons in the $\pm \mathbf{Q}'$ points, while the cone has finite density only in one of them, continuous transition between these two states at finite condensate density (that is, at any $h < h_{\text{sat}}$) is *not possible*. At infinitesimally small condensate density, *i.e.* at $h = h_{\text{sat}}$, direct transition is possible - it occurs at point D, which is a point of extended $O(2) \times O(2) \times O(2)$ symmetry: the two $O(2)$'s are phase symmetries while the third one is an emergent symmetry associated with the invariance of the potential energy at the constant total condensate density, $\rho = \rho_1 + \rho_2$, with respect to the distribution of condensate densities $\rho_{j=1,2} = \Psi_j^\dagger \Psi_j$ between the $\pm \mathbf{Q}'$ momenta. Large- S calculation of ladder diagrams which describe quantum corrections to the condensate energy place point D at $\delta = 2.91$ ⁵². Assuming that the first order transition does not realize, we are forced to conclude that V and cone states must be separated by the intermediate phase, occupying DBbC₂ region. This phase breaks the $O(2)$ symmetry between ρ_1 and ρ_2 and interpolates smoothly between the symmetric situation $\rho_1 = \rho_2$, on the D-B line, and the asymmetric one $\rho = \rho_1$ and $\rho_2 = 0$ (or vice versa) on the line D-C₂. In doing so the momentum of the 'minority' condensate is found to evolve continuously from the initial $\mathbf{q}_2 = \mathbf{Q}'$ (which coincides with the momentum of the 'majority' condensate ρ_1) on the line D-C₂ to the final $\mathbf{q}_2 = -\mathbf{Q}'$ on the D-B line⁵². The resulting phase is a non-coplanar one, with strongly pronounced asymmetry in the $x - y$ plane: $\langle S_{\mathbf{r}}^+ \rangle = \sqrt{\rho_1} e^{i\theta_1} e^{i\mathbf{Q}' \cdot \mathbf{r}} + \sqrt{\rho_2} e^{i\theta_2} e^{i\mathbf{q}_2 \cdot \mathbf{r}}$. The state is characterized by the broken $O(2) \times O(2) \times Z_2$. For the lack of better term we call it *double spiral*⁵².

Going down along the field axis takes us toward the dashed B-b-C₂ line below which, according to the analysis summarized in item (c) above, represents a phase with broken $Z_3 \times Z_2 \times O(2)$. Hence along this line Z_3 is replaced by $O(2)$, which makes it a continuation of the C-IC transitions line H-B.

(g) *low-field region*, $0 \leq h \ll h_{c1}(\delta)$. Semiclassical analysis at zero field $h = 0$ is well established and predicts incommensurate spiral state with zero total magnetization $M = 0$ of course. Quantum fluctuations renormalize strongly parameters of the spin spiral⁵⁴. The most quantum case of the spin $S = 1/2$ remains not fully understood even for the relatively weak deformation of exchanges $R = J - J' \leq J$ and is described in more details in Section III C.

At $\delta = 0$ one again has commensurate three-sublattice antiferromagnetic state, widely known as a 120° structure, which evolves into commensurate Y state in external magnetic field $h \neq 0$. Phenomenological analysis of Ref.47, Section III E, shows Y state becomes incommensurate when the deformation R exceeds $R_c \sim h^{3/2}$. Analysis near h_{c1} , reported in (b), tells that C-IC transition line must end up at point A. Comparing the energies of the incommensurate coplanar Y and the incommensurate umbrella state in the limit of vanishing magnetic field $h \rightarrow 0$, described in⁵⁰, identifies point E at $\delta = 1.1$ and $h = 0$ as the point of the transition between the $O(2) \times O(2)$ [the incommensurate coplanar V] and the $O(2) \times Z_2$ [the incommensurate cone] breaking states. Thus point E is analogous to point D.

By the arguments similar to those in part (f) above, there must be an intermediate phase with broken $O(2) \times O(2) \times Z_2$. It occupies region E-C₁-a-A in Figure 5. The state between A-C₁ and A-a-C₁ lines is characterized by different broken symmetries (see item (b) above) which makes the line A-a-C₁ to be the line of the $Z_3 \rightarrow O(2)$ transition. It thus has to be viewed as a continuation of the CIT line O-A.

To summarize, the quasi classical phase diagram in Figure 5 contains many different phases. It worth keeping in mind that it has been obtained under assumption of *continuous* phase transitions between states with different orders. Several of the shown there phase boundaries are tentative – their existence is conjectured based on different symmetry properties of the states they are supposed to separate. To highlight their conjectured nature, such lines are drawn *dashed* in Figure 5. These include line B-b-C₂ which separates distorted umbrella (with broken $Z_3 \times O(2) \times Z_2$) and double spiral (with broken $O(2) \times O(2) \times Z_2$), and similar to it line A-a-C₁ located right below the UUD phase. The end-points of these dashed lines are conjectured to be C₂ and C₁, correspondingly, which are the points of the two-magnon condensation [item (e)]. Line D-C₂, separating phases with broken $O(2) \times O(2) \times Z_2$ and $O(2) \times Z_2$, established via high-field analysis in item (f), is conjectured to end at the same C₂. Since different behavior cannot be ruled out at the present, its extension to the near-plateau region is indicated by the dashed line as well. Similar arguments apply to the line E-C₁. Finally, line C₂-C-C₁, covering the very tip of the UUD plateau phase, is made dashed because it is located past the two-magnon condensation transition (line C₁-C₂) into the spin-nematic state instabilities of which have not been explored in sufficient details yet.

One of the most unexpected and remarkable conclusions emerging from the analysis summarized here is the identification of the continuous line of C-IC transitions (line H-B-b-C₂-C-C₁-a-A-O), separating phases with discrete Z_3 from those with continuous $O(2)$ symmetry. Its existence owes to the non-trivial interplay between geometric frustration and quantum spin fluctuations in the triangular antiferromagnet.

Spin excitation spectra: Many of the ordered *non-collinear* states described above harbor spin excitations with rather unusual characteristics. It has been pointed out some time ago^{55,56} that local non-collinearity of the magnetic order results in the strong renormalization of the spin wave spectra at $1/S$ order. (This should be contrasted with the case of the collinear magnetic order, where quantum corrections to the excitation spectrum appear only at $1/S^2$ order.) This interesting effect, reviewed in⁵⁷, is responsible for dramatic flattening of spin wave dispersion and/or appearance of ‘roton-like’ minima and related thermodynamic anomalies at temperatures as low as $0.1 - 0.2J$ ^{58,59}.

C. Spin 1/2 spatially anisotropic triangular antiferromagnet with $J' \neq J$

We now turn to the case of most quantum system: a spin 1/2 antiferromagnet. Qualitatively, one expects quantum fluctuations to be most pronounced in this case, which suggests,

in line with ‘order-by-disorder’ arguments of Section III A, a selection of the ordered Y, UUD and V states at and near the isotropic limit $J' \approx J$. Behavior away from this isotropic line represents a much more difficult problem, mainly due to the absence of physically motivated small parameter, which would allow for controlled analytical calculations. Aside from the two limits where small parameters do appear, namely the high field region near the saturation field and the limit of weakly coupled spin chains (see below), the only available approach is numerical.

Most of recent numerical studies of triangular lattice antiferromagnets focus on the zero field limit, $h = 0$, and on the phase diagram as a function of the ratio J'/J . These studies agree that a two-dimensional magnetic spiral order, well established at the isotropic $J' = J$ point, becomes incommensurate with the lattice when $J' \neq J$ and persists down to approximately $J' = 0.5J$. The ordering wave vector of the spiral \mathbf{Q}' is strongly renormalized by quantum fluctuations^{54,60} away from the semiclassical result. Below about $J' = 0.5J$, strong finite size effects and limited numerical accuracy of the exact diagonalization⁶¹ and DMRG^{60,62} methods does not allow one to obtain a definite answer about the ground state of the spin-1/2 $J - J'$ Heisenberg model.

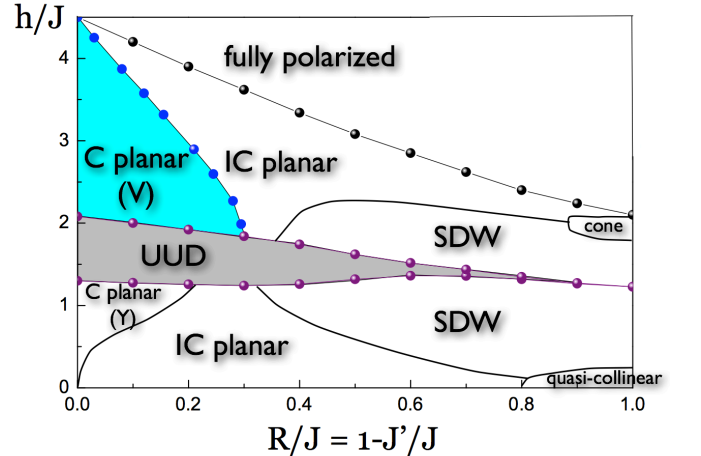


FIG. 7: Phase diagram of the spin $S = 1/2$ spatially anisotropic triangular antiferromagnet in magnetic field. Vertical axis - magnetic field h/J , horizontal - dimensionless degree of spatial anisotropy, $R/J = 1 - J'/J$. Notation C/IC stands for commensurate/incommensurate phases, correspondingly. Adapted from Chen *et al.*, Phys. Rev. B 87, 165123 (2013).

This unexpected behavior is a direct consequence of the strong frustration inherent in the triangular geometry. In the $J' \ll J$ limit the lattice decouples into a collection of linear spin chains weakly coupled by the frustrated interchain exchange $\mathcal{H}' = J' \sum_{x,y} \mathbf{S}_{x,y} \cdot (\mathbf{S}_{x-1/2,y+1} + \mathbf{S}_{x+1/2,y+1})$. Even classically, spin-spin correlations between spins from different chains are strongly suppressed as can be seen from the limit $J'/J \rightarrow 0$ when classical spiral wave vector $Q'_x = 2 \cos^{-1}[-J'/2J] \rightarrow \pi + J'/J$. In this limit the relative angle between the spin at (integer-numbered) site x of the y -th chain and its neighbor at (half-integer-numbered) $x + 1/2$ site of the

$y + 1$ -th chain approaches $\pi/2 + J'/(2J)$. Thus the scalar product of two classical spins at neighboring chains vanishes as $J'/(2J) \rightarrow 0$.

Quantum spins adds strong quantum fluctuations to this behavior, resulting in the numerically observed near-exponential decay of the inter-chain spin correlations, even for intermediate value $J'/J \lesssim 0.5$ ^{60,62}. While some of the studies interpret such effective decoupling as the evidence of the spin-liquid ground state^{61,62}, the others conclude that the coplanar spiral ground state persists all the way to $J' = 0$ ^{60,63}.

Analytical renormalization group approach⁶⁴, which utilizes symmetries and algebraic correlations of low-energy degrees of freedom of individual spin-1/2 chains, finds that the system experiences quantum phase transition from the ordered spiral state to the unexpected collinear antiferromagnetic (CoAF) ground state. This novel magnetically ordered ground state is stabilized by strong quantum fluctuations of critical spin chains. This finding is supported by the coupled-cluster study^{65,66}, functional renormalization group⁶⁷ as well as by the combined DMRG and analytical RG studies in⁶⁸. It is fair to say that more studies of the very difficult $J'/J \rightarrow 0$ limit of the spatially anisotropic triangular model are highly desirable in order to definitively sort out the issue of the ultimate ground state.

Having described the limiting behavior along $h = 0$ and $J' = J$ ($R = 0$) axes, we now discuss the full $h - R$ phase diagram of the spin-1/2 Heisenberg model shown in Figure 7 ($R = J - J'$). The diagram is derived from extensive DMRG study of triangular cylinders (spin tubes) composed of 3, 6 and 9 chains and of lengths 120 - 180 sites (depending on R and the magnetization value) as well as detailed analytical RG arguments applicable in the limit $J' \ll J$ ⁴⁷. It compares well, in the regions of small and intermediate R , with the variational and exact diagonalization study by Tay and Motrunich⁴⁵. The comparison is less conclusive in the regime of large anisotropy, $R \rightarrow 1$, which is most challenging for numerical techniques as already discussed above. (The biggest uncertainty of the diagram in Figure 7 consists in so far undetermined region of stability of the cone phase and, to a lesser degree, the phase boundaries between incommensurate (IC) planar and SDW phases.)

The main features of the phase diagram of the quantum spin-1/2 model are:

(1) High-field incommensurate coplanar (incommensurate V or fan) phase, which is characterized by the broken $O(2) \times O(2)$ symmetry, is stable for *all* values of the exchange anisotropy $1 \geq R \geq 0$. This novel analytical finding, confirmed in DMRG simulations, is described in Ref.47. This result is specific to the quantum $S = 1/2$ model – for any other value of the site spin $S \geq 1$ there is a quantum phase transition between the incommensurate planar and the incommensurate cone phases at some R_S . The critical value R_S is spin-dependent and decreases monotonically with S . We find $R_S \approx 0.9, 0.5, 0.4$ for $S = 1, 3/2, 2$, respectively⁴⁷.

(2) 1/3 Magnetization plateau (UUD phase) is present for all values of R too: it extends from $R = 0$ all the way to $R = 1$. This striking conclusion is based on analytical calculations near the isotropic point⁵⁰, discussed in the previous

Section, complementary field-theoretical calculations near the decoupled chains limit of $R \approx 1$ ^{47,69} and on extensive DMRG studies of the UUD plateau in Ref.47.

(3) A large portion of the diagram in Figure 7, roughly to the right of $R = 0.5$, is occupied by the novel incommensurate collinear SDW phase. Physical properties of this magnetically ordered and yet intrinsically quantum state are summarized in Section IV A below.

Comparing the quantum phase diagram in Figure 7 with the previously described large- S phase diagram in Figure 5, one notices that both the high-field incommensurate coplanar and the UUD phases are present there too. The fact that both of these states become *more stable* in the spin-1/2 case and expand to the whole range of exchange anisotropy $0 < R < 1$, represents a striking *quantitative* difference between the large- S and $S = \frac{1}{2}$ cases. It should also be noticed that both phase diagrams demonstrate that the range of stability of the incommensurate cone (umbrella) phase is greatly diminished.

In contrast, a collinear SDW phase, which occupies a good portion of the quantum phase diagram in Figure 7, is not present in Figure 5 at all - and this constitutes a major qualitative distinction between the large- S and the quantum $S = \frac{1}{2}$ cases.

IV. SDW AND NEMATIC PHASES OF SPIN-1/2 MODELS

A. SDW

The *collinear SDW phase* is characterized by the *modulated* expectation value of the local magnetization

$$\langle S_{\mathbf{r}}^z \rangle = M + \text{Re}[\Phi e^{i\mathbf{k}_{\text{sdw}} \cdot \mathbf{r}}], \quad (8)$$

where Φ is the SDW order parameter, and SDW wave vector \mathbf{k}_{sdw} is generally incommensurate with the lattice and, moreover, is the function of the uniform magnetization M and anisotropy R . Eq.(8) is very unusual for a classical (or semi-classical) spin system, where magnetic moments tend to behave as vectors of fixed length. It is, however, a relatively common phenomenon in itinerant electron systems with nested Fermi surfaces⁷⁰⁻⁷². The appearance of such a state in a *frustrated* system of coupled spin-1/2 chains is rooted in a deep similarity between Heisenberg spin chain and one-dimensional spin-1/2 Dirac fermions⁷³⁻⁷⁵: thanks to the well-known phenomenon of one-dimensional spin-charge separation, the spin sectors of these two models are identical. Ultimately, it is this correspondence that is responsible for the ‘softness’ of the amplitude-like fluctuations underlying the collinear SDW state of Figure 7.

Figure 8 schematically shows a dispersion of $S = 1/2$ electron in a magnetic field. Fermi-momenta of up- and down-spin electrons $k_{\uparrow/\downarrow}$ are shifted from the Fermi momentum of non magnetized chain, $k_F = \pi/2$, by $\pm \Delta k_F = \pm \pi M$, where M is the magnetization. As a result, the momentum of the *spin-flip* scattering processes, which determine transverse spin correlation function $\langle S^+ S^- \rangle$, is given by $\pm(k_{\uparrow} - (-k_{\downarrow})) = \pm 2k_F = \pm \pi$, and remains commensurate

with the lattice. At the same time, longitudinal spin excitations, which preserve S^z , now involve momenta $\pm 2k_{\uparrow/\downarrow} = \pi(1 \pm 2M)$ and become incommensurate with the lattice. To put it differently, in the magnetized chain with $M \neq 0$ low-energy longitudinal spin fluctuations can be parameterized as $S^z(x) \sim S^z e^{i(\pi-2\pi M)x} + S^{z*} e^{i(-\pi+2\pi M)x}$, where (calligraphic) $S^z(x)$ represents slow (low-energy) longitudinal mode. Similarly, transverse spin fluctuations are written as $S^+(x) \sim S^+ e^{i\pi x}$, with S^+ representing low-energy transverse mode.

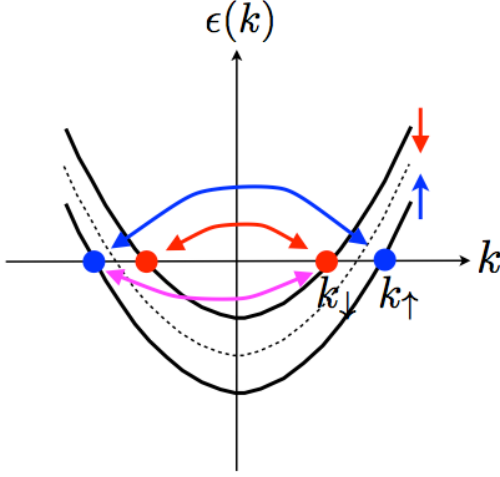


FIG. 8: Schematics of spinon dispersion for one-dimensional spin chain in magnetic field. Dashed line shows dispersion for zero field. $k_{\uparrow}(k_{\downarrow})$ denote Fermi momentum of spin 'up' ('down') spinons correspondingly. Fermi momentum in the absence of the field is $k_F = \pi/2$.

This simple fact has dramatic consequences for frustrated interchain interaction $\mathcal{H}' = J' \sum_{x,y} \mathbf{S}_{x,y} \cdot (\mathbf{S}_{x-1/2,y+1} + \mathbf{S}_{x+1/2,y+1})$. Longitudinal (z) component of the sum of two neighboring spins on chain ($y+1$) adds up to $S_{x-1/2,y+1}^z + S_{x+1/2,y+1}^z \rightarrow \sin[\pi M](S_{x,y+1}^z e^{i(\pi-2\pi M)x} + \text{h.c.})$, while the sum of their transverse components becomes a *derivative* of the smooth component of the transverse field S^+ , $S_{x-1/2,y+1}^+ + S_{x+1/2,y+1}^+ \rightarrow e^{i\pi x} \partial_x S_{x,y+1}^+$. Hence the low-energy limit of the inter-chain interaction reduces to $\mathcal{H}' \rightarrow \sum_y \int dx \{ J' \sin[\pi M] S_{x,y}^{z*} S_{x,y+1}^z + J' S_{x,y}^- \partial_x S_{x,y+1}^+ + \text{h.c.} \}$. The presence of the spatial derivative in the second term severely weakens it⁶⁹ and results in the domination of the density-density interaction (first term) over the transverse one (second term). The field-induced shift of the Fermi-momenta from its commensurate value, $k_F \rightarrow k_{\uparrow/\downarrow}$, together with frustrated geometry of inter-chain exchanges, are the key reasons for the field-induced stabilization of the two-dimensional longitudinal SDW state.

Symmetry-wise, the SDW state breaks no global symmetries (time reversal symmetry is broken by the magnetic field, which also selects the z axis), and, in particular, it preserves $U(1)$ symmetry of rotations about the field axis. This crucial feature implies the absence of the off-diagonal magnetic or

der $\langle S_{\mathbf{r}}^{x,y} \rangle = 0$ and would be gapless (Goldstone) spin waves. Instead, SDW breaks lattice translational symmetry. Its order parameter $\Phi \sim \langle S^z \rangle \neq 0$ is determined by inter-chain interactions^{69,76}. Provided that $\mathbf{k}_{\text{sdw}} = \pi(1 - 2M)\hat{x}$ is *incommensurate* with the lattice, the only low energy mode is expected to be the pseudo-Goldstone acoustic mode of broken translations, known as a *phason*. (Inter-chain interactions do affect \mathbf{k}_{sdw} but in the limit of small J'/J this can be neglected.) The phason is a purely longitudinal mode corresponding to the phase of the complex order parameter Φ and hence represents a modulation of S^z only. This too is unusual in the context of insulating magnets, where, typically, the low energy collective modes are *transverse* spin waves, associated with small rotations of the spins away from their ordered axes. In the spin wave theory, longitudinal modes are typically expected to be highly damped^{57,77,78}, and hence hard to observe. (For a recent notable exception to this rule see a study of amplitude-modulated magnetic state of PrNi_2Si_2 ⁷⁹.) In the SDW state, the longitudinal phason mode is the only low energy excitation. Transverse spin excitations, which SDW also supports, have a finite spectral gap. This, in fact, is one of key experimentally identifiable features of the SDW phase. More detailed description of spin excitations of this novel phase, as well as of the spin-nematic state reviewed below, can be found in the recent study⁷⁶.

At present, there are three known routes to the field-induced longitudinal SDW phase for a quasi-one-dimensional system of weakly coupled spin chains. The first, reviewed above, relies on the geometry-driven frustration of the transverse inter-chain exchange, which disrupts usual transverse spin ordering and promotes incommensurate order of longitudinal S^z components. The other route, described in the subsection IV A 1 below, relies on Ising anisotropy of individual chains. Lastly, it turns out that a two-dimensional SDW state may also emerge in a system of weakly coupled *nematic* spin chains - this unexpected possibility is reviewed in the subsection IV B.

1. SDW in a system of Ising-like coupled chains

There is yet another surprisingly simple route to the two-dimensional SDW phase. It consists in replacing Heisenberg chains with XXZ ones with pronounced Ising anisotropy. It turns out that a sufficiently strong magnetic field, applied along the z (easy) axis, drives individual chains into a critical Luttinger liquid state with dominant *longitudinal*, $S^z - S^z$, correlations⁸⁰. This crucial property ensures that weak residual inter-chain interaction selects incommensurate longitudinal SDW state as the ground state of the anisotropic two-dimensional system.

We note, for completeness, that not every field-induced gapless spin state is characterized by the dominant longitudinal spin correlations. For example, another well-known gapped system, spin-1 Haldane chain, can too be driven into a critical Luttinger phase by sufficiently strong magnetic field⁸¹⁻⁸⁴. However, that critical phase is instead dominated by strong transverse spin correlations^{85,86}. As a result, a 2d

ground state of weakly coupled spin-1 chains is a usual cone state⁸⁷.

2. Magnetization plateau as a commensurate collinear SDW phase

The *commensurate* case, when the wavelength $\lambda_{\text{sdw}} = 2\pi/k_{\text{sdw}}$ is a rational fraction of the lattice period, $\lambda_{\text{sdw}} = q/p$, requires special consideration. (Here the lattice period is set to be 1 and q and p are integer numbers.) Such commensurate state is possible at commensurate magnetization values $M^{(p,q)} = \frac{1}{2}(1 - \frac{2q}{p})$. At these values, ‘sliding’ SDW state locks-in with the lattice, resulting in the loss of continuous translational symmetry. The SDW-plateau transition is then an incommensurate-commensurate transition of the sine-Gordon variety^{47,69}.

It turns out that in two-dimensional triangular lattice such locking is possible, provided that integers p and q have the same parity (both even or both odd)⁶⁹ (and, of course, provided that the spin system *is* in the two-dimensional collinear SDW phase). This condition selects $M = 1/3 M_{\text{sat}}$ plateau ($q = 1, p = 3$) as the most stable one, in a sense of the biggest energy gap with respect to creation of spin-flip excitation (which changes total magnetization of the system by ± 1). The next possible plateau is at $M = 3/5 M_{\text{sat}}$ ($q = 1, p = 5$)⁶⁹ – however this one apparently does not realize in the phase diagram in Figure 7, perhaps because it is too narrow and/or happen to lie inside the (yet not determined numerically) cone phase.

Applied to the one-dimensional spin chain, the above condition can be re-written as a particular $S = \frac{1}{2}$ version of the Oshikawa-Yamanaka-Affleck condition^{88,89} for the period- p magnetization plateau in a spin- S chain, $pS(1 - M/M_{\text{sat}}) = \text{integer}$. Interestingly, this shows that $p = 3$ plateau at $M = 1/3 M_{\text{sat}}$ of the total magnetization M_{sat} is possible for all values of the spin S : the quantization condition becomes simply $2S = \text{integer}$. This rather non-obvious feature has in fact been numerically confirmed in several extensive studies^{90–92}.

B. Spin nematic

Spin nematic represents another long-sought type of exotic ordering. Out of many possible nematic states^{93,94}, our focus here is on bond-nematic order associated with the two-magnon pairing⁹⁵ and the appearance of the non-local order parameter $Q_{--} = S_{\mathbf{r}}^- S_{\mathbf{r}'}^-$ defined on the $\langle \mathbf{r}, \mathbf{r}' \rangle$ bond connecting sites \mathbf{r} and \mathbf{r}' . Such order parameter can be build from quadrupolar operators $Q_{x^2-y^2} = S_{\mathbf{r}}^x S_{\mathbf{r}'}^x - S_{\mathbf{r}}^y S_{\mathbf{r}'}^y$ and $Q_{xy} = S_{\mathbf{r}}^x S_{\mathbf{r}'}^y + S_{\mathbf{r}}^y S_{\mathbf{r}'}^x$, as $Q_{--} = Q_{x^2-y^2} - iQ_{xy}$ ⁹⁶. This bond-nematic order is possible in both $S \geq 1$, where quadrupolar order was originally suggested⁹⁷, and $S = 1/2$ systems of localized spins, coupled by exchange interaction.

The magnon pairing viewpoint, explored in great length in^{96,98,99}, is extremely useful for understanding basic properties of the spin-nematic state: the nematic can be thought of as a ‘bosonic superconductor’ formed as a result of two-magnon

condensation $\langle S_{\mathbf{r}}^- S_{\mathbf{r}'}^- \rangle = \langle Q_{--} \rangle \neq 0$. As in a superconductor, a two-magnon condensate breaks $U(1)$ symmetry, which in this case is a breaking of the spin rotational symmetry with respect to magnetic field direction. It does not, however, break time-reversal symmetry (which requires a single-particle condensation). Just as in a superconductor, single-particle excitations of the nematic phase are gapped. This implies that transverse spin correlation function $\langle S_{\mathbf{r}}^+ S_{\mathbf{0}}^- \rangle \sim e^{-r/\xi}$, which probes single magnon excitations, is short-ranged and decays exponentially. At the same time, fluctuations of magnon density, which are probed by longitudinal spin correlation function $\langle S_{\mathbf{r}}^z S_{\mathbf{0}}^z \rangle$, are sound-like acoustic (Bogoliubov) modes.

1. Weakly coupled nematic chains

Basic ingredients of this picture - gapped magnon excitations and attractive interaction between them - are nicely realized in the spin-1/2 quasi-one-dimensional material LiCuVO_4 , reviewed in Section VB: the gap in the magnon spectrum is caused by the strong external magnetic field h which exceeds (single-particle) condensation field $h_{\text{sat}}^{(1)}$, while the attraction between magnons is caused by the *ferromagnetic* (negative) sign of exchange interaction J_1 between the nearest spins of the chain. Under these conditions, the two-magnon bound state, which lies below the gapped single particle states, condenses at $h_{\text{sat}}^{(2)}$, which is higher than $h_{\text{sat}}^{(1)}$. As a result, a spin nematic state is naturally realized in each individual chain in the intermediate field interval $h_{\text{sat}}^{(1)} < h < h_{\text{sat}}^{(2)}$.

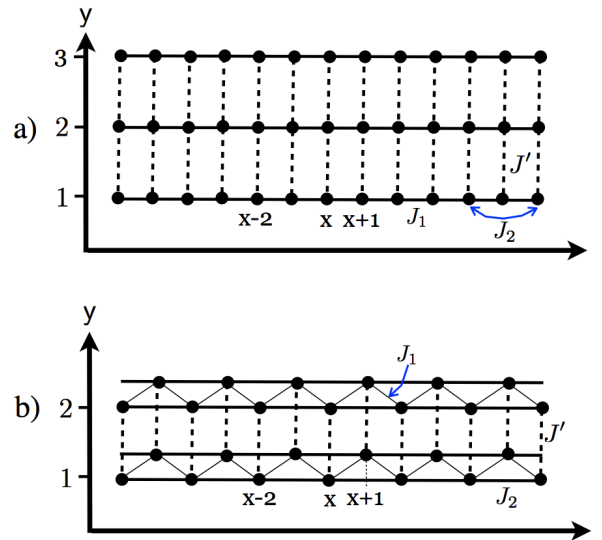


FIG. 9: (a) Weakly coupled nematic chains with ferromagnetic J_1 (solid lines) and antiferromagnetic next-nearest J_2 , coupled by an inter-chain exchange J' . (b) Same system viewed as a set of weakly coupled zig-zag chains.

Note, however, that a true $U(1)$ symmetry breaking is not possible in a single chain, where instead a critical Luttinger state with algebraically decaying nematic correlations

is established⁹⁶. To obtain a true *two-dimensional nematic* phase, one needs to establish a phase coherence between the phases of order parameters $Q_{--}(y)$ of different chains. By our superconducting analogy, this requires a Josephson coupling to transfer (hop) bound two-magnon pairs between nematic chains. The corresponding ‘hopping’ term reads $K \sum_{x,y} (Q_{++}(x,y)Q_{--}(x,y+1) + \text{h.c.})$. Microscopically, such an interaction represents a four-spin coupling, which is not expected to be particularly large in a good Mott insulator with a large charge gap, such as LiCuVO_4 . However, even if K is absent microscopically, it will be generated perturbatively from the usual inter-chain spin exchange $J' \sum_{x,y} (S_{x,y}^+ S_{x,y+1}^- + \text{h.c.})$, which plays the role of a single-particle tunneling process in the superconducting analogy. (Observe that expectation value of this interaction in the chain nematic ground state is zero – adding or removing of a single magnon to the ‘superconducting magnon’ ground state is forbidden at energies below the single magnon gap.) The pair-tunneling generated by fluctuations is estimated to be of the order $K \sim (J')^2/J_1 \ll J'$.

At the same time, $S^x - S^z$ interaction between chains does not suffer from a similar ‘low-energy suppression’. This is because S^z is simply proportional to a number of magnon pairs, $n_{\text{pair}}(x,y) = 2n(x,y)$, which is just twice the magnon number $n(x,y)$. Hence $S^z(x,y) = 1/2 - 2n(x,y)$ differs only a by coefficient 2 from its usual expression in terms of magnon density.

We thus have a situation where the strength of interchain density-density ($S^x - S^z$) interaction, which is determined by the original interchain J' , is much stronger than that for the fluctuation-generated Josephson interaction $K \sim (J')^2/J_1$. In addition, more technical analysis of the scaling dimensions of the corresponding operators shows⁷⁶, that the two competing interactions are characterized by (almost) the same scaling dimension (approximately equal to 1 for $h \approx h_{\text{sat}}$) which makes them both strongly relevant in the renormalization group sense. Given an inequality $J' \gg (J')^2/J_1$, which selects interchain $S^x - S^z$ interaction as the strongest one, we end up with a *two-dimensional collinear SDW phase* build out of nematic spin chains^{76,100}. This conclusion holds for all h except for the immediate vicinity of the saturation field $h_{\text{sat}}^{(2)}$. There a separate fully two-dimensional BEC analysis is required, due to the vanishing of spin velocity at the saturation field, and the result is a true *two-dimensional nematic phase* in the narrow field range $h_{\text{sat}}^{(1)} \lesssim h \leq h_{\text{sat}}^{(2)}$ ^{76,99,100}. A useful analogy to this competition is provided by models of striped superconductors, where the competition is between the superconducting order (a magnetic analogue of which is the spin nematic) and the charge-density wave order (a magnetic analogue of which is the collinear SDW), see Ref.101 and references therein.

To summarize, weak inter-chain interaction J' between $J_1 - J_2$ spin chains with strong nematic spin correlations actually stabilizes a two-dimensional SDW phase as the ground state in a wide range of magnetization. This state preserves $U(1)$ symmetry of spin rotations and is characterized by short-range transverse spin correlations, similar to a nematic state.

2. Spin-current nematic state at the 1/3-magnetization plateau

The discussion in the previous Subsection was focused on the systems with ferromagnetic exchange ($J_1 < 0$) on some of the bonds – as described there, negative exchange needed in order to obtain an *attractive* interaction between magnons.

Superconducting analogy, extensively used above, forces one to ask, by analogy with superconducting states of repulsive fermion systems (such as, for example, pnictide superconductors or high-temperature cuprate ones), if it is possible to realize a spin-nematic in a spin system with only antiferromagnetic (that is, repulsive) exchange interactions between magnons. To the best of our knowledge, the first example of such a state is provided by the spin-current state described in part (e) of the Section III B. Being nematic, this state is characterized by a spin current long-range order and the absence of the magnetic long-range order in the transverse to the magnetic field direction⁵¹.

A very similar state, named *chiral Mott insulator*, was recently discovered in the variational wave function study of a two-dimensional system of interacting bosons on frustrated triangular lattice¹⁰² as well as in a one-dimensional system of bosons on frustrated ladder^{103,104}. In both cases, a chiral Mott insulator is an intermediate phase, which separates the usual Mott insulator state (which is a boson’s analogue of the UUD state) from the superfluid one (which is an analogue of the cone state). As in Figure 5, it intervenes between the states with distinct broken symmetries (Z_3 and $O(2) \times Z_2$ in our case), and gives rise to two continuous transitions instead of a single discontinuous one.

C. Magnetization plateaus in itinerant electron systems

Up-up-down magnetization plateaus, found in the triangular geometry, are of classical nature. Over years, several interesting suggestions of non-classical (liquid-like) magnetization plateaux have been put forward^{105–110}, but so far not observed in experiments or numerical simulations. Very recently, however, two numerical studies^{111,112} of the spin-1/2 kagomé antiferromagnet have observed non-classical magnetization plateaux at $M/M_{\text{sat}} = 1/3, 5/9, 7/9$. These intriguing findings, taken together with earlier prediction of a *collinear spin liquid* at $h = h_{\text{sat}}/3$ in the classical kagomé antiferromagnet¹¹³, hint at a very rich magnetization process of the quantum model, the ground state of which at $h = 0$ is a Z_2 spin liquid⁴.

A different point of view on the magnetization plateau was presented recently in Ref.114. The authors asked if the plateau is possible in an itinerant system of weakly-interacting electrons. The answer to this question is affirmative, as can be understood from the following consideration.

Let us start with a system of non-interacting electrons on a triangular lattice. A magnetic field, applied in-plane in order to avoid complications due to orbital effects, produces magnetization $M = (n_{\uparrow} - n_{\downarrow})/2$, where densities n_{σ} of electrons with spin $\sigma = \uparrow, \downarrow$ are constrained by the total density $n = n_{\uparrow} + n_{\downarrow}$. Consider now special situation with $n_{\uparrow} = 3/4$,

at which the Fermi-surface of $\sigma = \uparrow$ electrons, by virtue of lattice geometry, acquires particularly symmetric shape: a hexagon inscribed inside the Brillouin zone hexagon, see Figure 10.

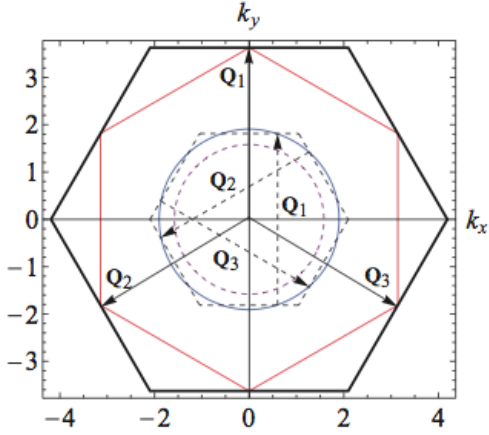


FIG. 10: The Fermi surface (red hexagon) of the non-interacting $\sigma = \uparrow$ electrons on a triangular lattice at $n_{\uparrow} = 3/4$. Nearly circular Fermi surface of the minority $\sigma = \downarrow$ electrons is shown by blue line. Bold black hexagon represents the Brillouin zone. Adapted from Zhihao Hao and Oleg A. Starykh, Phys. Rev. B 87, 161109 (2013).

Points where $\sigma = \uparrow$ Fermi-surface touches the Brillouin zone (denoted by vectors $\pm \mathbf{Q}_j$ with $j = 1, 2, 3$ in Fig.10) are the van Hove points, at which Fermi-velocity vanishes and electron dispersion becomes quadratic. They are characterized by the logarithmically divergent density of states. In addition, being a hexagon, $\sigma = \uparrow$ Fermi-surface is perfectly nested. As a result, static susceptibility $\chi_{\uparrow}(\mathbf{k})$ of spin-up electrons is strongly divergent, as $\log^2(|\mathbf{k} - \mathbf{Q}_j|)$, for wave vectors $\mathbf{k} \approx \mathbf{Q}_j$.

Given this highly susceptible spin- \uparrow Fermi surface, it is not surprising that a weak interaction between electrons, either in the form of a direct density-density interaction $V n_{\mathbf{r},\uparrow} n_{\mathbf{r}+\delta_j}$ between electrons on, e.g., nearest sites, or in the form of a local Hubbard interaction $U n_{\mathbf{r},\uparrow} n_{\mathbf{r},\downarrow}$ between the majority and minority particles, drives spin- \uparrow electrons into a gapped correlated state - the charge density wave (CDW) state¹¹⁴ with fully gapped Fermi surface. Moreover, CDW ordering wave vectors \mathbf{Q}_j are commensurate with the lattice, leading to a commensurate CDW for the spin- \uparrow electrons¹¹⁵.

Minority spin- \downarrow electrons experience position-dependent effective field $U \langle n_{\mathbf{r},\uparrow} \rangle$ and form CDW as well. Depending on whether or not vectors \mathbf{Q}_j span the spin-down Fermi-surface (this depends on n_{\downarrow} density), the Fermi-surface of $\sigma = \downarrow$ electrons may or may not experience reconstruction. However, being not nested, it is guaranteed to retain at least some parts of the critical Fermi-surface.

The resulting state is a co-existence of a charge- and collinear spin-density waves, together with critical $\sigma = \downarrow$ Fermi surface. Since the energy cost of promoting a spin- \downarrow electron to a spin- \uparrow state is finite (and given by the gap on the

spin- \uparrow Fermi surface), the resulting state realizes *fractional* magnetization plateau, the magnetization of which is determined by the total density n via $M = (3/2 - n)/2$. At half-filling, $n = 1$, the plateau is at $1/2$ of the total magnetization, but for $n \neq 1$ it takes a fractional value. Amazingly, the obtained state is also a *half-metal*¹¹⁶ - the only conducting band is that of (not gapped) minority spin- \downarrow electrons.

Theoretical analysis sketched here bears strong similarities with recent proposals^{115,117-120} of collinear and chiral spin-density wave (SDW) and superconducting states of itinerant electrons on a honeycomb lattice in the vicinity of electron filling factors $3/8$ and $5/8$ at zero magnetization. Our analysis shows that even simple square lattice may host similar half-metallic magnetization plateau state, see supplement to¹¹⁴. Similar to the case of a magnetic insulator, described in the previous Sections, external magnetic field sets the direction of the collinear CDW/SDW state. The resulting half-metallic state only breaks the discrete translational symmetry of the lattice, resulting in fully gapped excitations, and remains stable to fluctuations of the order parameter about its mean-field value. In addition to standard solid state settings, the described phenomenon may also be observed in experiments on cold atoms, where desired high degree of polarization can be easily achieved¹²¹. It appears that, in addition to the half-metallic state, the system may also support p-wave superconductivity - a competition between these phases may be efficiently studied with the help of functional renormalization group¹²².

V. EXPERIMENTS

Much of the current theoretical interest in quantum antiferromagnetism comes from the amazing experimental progress in this area during the last decade. The number of interesting materials is too large to review here, and for this reason we focus on a smaller sub-set of recently synthesized quantum spin-1/2 antiferromagnets, which realize some of quantum states discussed above.

One of the best known among this new generation of materials is Cs_2CuCl_4 , extensively studied by Coldea and collaborators in a series of neutron scattering experiments¹²³⁻¹²⁵ and by others via NMR¹²⁶ and, more recently, ESR¹²⁷⁻¹³⁰ experiments. This spin-1/2 material represents a realization of a deformed triangular lattice with $J'/J = 0.34$ ¹²⁴ and significant DM interactions on chain and inter-chain (zig-zag) bonds, connecting neighboring spins^{69,124}. Inelastic neutron scattering experiments have revealed unusually strong multi-particle continuum, the origin of which has sparked intense theoretical debate¹³¹⁻¹³⁸. The current consensus is that Cs_2CuCl_4 is best understood as a weakly-ordered quasi-one-dimensional antiferromagnet, whose spin excitations smoothly interpolate from fractionalized spin-1/2 spinons of one-dimensional chain at high- and intermediate energies to spin waves at lowest energy ($\ll J'$)¹³⁸. Although weak, residual inter-plane and DM interactions play the dominant role in the magnetization process of this material. The resulting $B - T$ phase diagram is rather complex and highly anisotropic¹³⁹, and does not con-

tain a magnetization plateau. However it is worth mentioning that this was perhaps the first spin-1/2 material, a magnetic response of which featured a SDW-like phase ordering wave vector, which scales *linearly* with magnetic field in an about 1 Tesla wide interval (denoted as phase “S” in¹²³ and as phase “E” in¹³⁹). While still not well understood, this experimental observation have provided valuable hint to quasi-1d approach based on viewing Cs_2CuCl_4 as a collection of weakly coupled spin chains¹³⁸.

A. Magnetization plateau

Robust 1/3 magnetization plateau – the first of its kind among triangular spin-1/2 antiferromagnets – is present in Cs_2CuBr_4 , which has the same crystal structure as Cs_2CuCl_4 , but is less deformed, $J'/J \approx 0.7$, and is more two-dimensional than the chloride-based material.

The observed plateau, which is about 1 Tesla wide ($h_{c1} = 13.1\text{T}$ and $h_{c2} = 14.4\text{T}$)^{140–142}, is clearly visible in both magnetization and elastic neutron scattering measurements^{141,142}, which determined the UUD spin structure on the plateau. The observation of the magnetization plateau has generated a lot of experimental activity. The quantum origin of the plateau visibly manifests itself via essentially temperature-independent plateau’s critical fields $h_{c1,2}(T) \approx h_{c1,2}(T = 0)$, as found in the thermodynamic study¹⁴³. This behavior should be contrasted with the phase diagram of the spin-5/2 antiferromagnet $\text{RbFe}(\text{MoO}_4)_2$ ^{27,144,145}, where the critical field $h_{c1}(T)$ does show strong downward shift with T . (Recall that in the classical model, Figure 3, the UUD phase collapses to a single point at $T = 0$.)

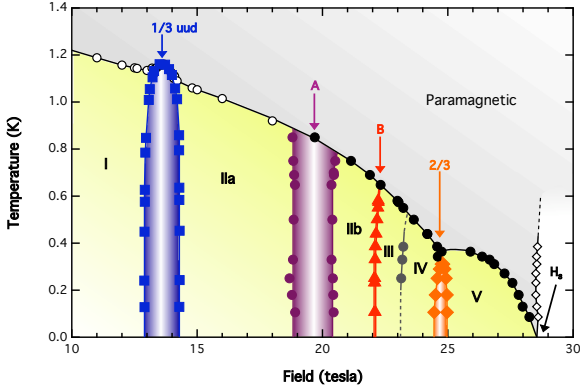


FIG. 11: Magnetic phase diagram of Cs_2CuBr_4 , as deduced from the magnetocaloric-effect data taken at various temperatures. Circles indicate second-order phase boundaries, whereas other symbols except the open diamonds indicate first-order boundaries. Adapted from Fortune *et al.*, Phys. Rev. Lett. 102, 257201 (2009).

Commensurate up-up-down spin structure of Cs_2CuBr_4 is also supported by NMR measurements^{146,147} which in addition finds that transitions between the commensurate plateau and adjacent to it incommensurate phases are discontinuous (first-order). Extensive magnetocaloric effect and magnetic-torque experiments¹⁴⁸ have uncovered surprising cascade of

field-induced phase transitions in the interval 10 – 30 T. The most striking feature of the emerging complex phase diagram is that it appears to contain up to 9 different magnetic phases – in stark contrast with the ‘minimal’ theoretical model diagram in Figure 3 which contains just 3 phases! This, as well as strong sensitivity of the magnetization curve to the direction of the external magnetic field with respect to crystal axis, strongly suggest that the difference in the phase diagrams has to do with spatial ($J' \neq J$) and spin-space (asymmetric DM interaction) anisotropies present in Cs_2CuBr_4 . Large- S and classical Monte Carlo studies²⁸ do find the appearance of new incommensurate phases in the phase diagram, in qualitative agreement with the large- S diagram of Figure 5 (note that the latter does not account for the DM interaction which significantly complicates the overall picture²⁸).

Perhaps the most puzzling of the “six additional” phases is a narrow region at about $B = 23\text{T}$, where dM/dB exhibits sharp double peak structure, interpreted in^{142,149} as a novel magnetization plateau at $M/M_{\text{sat}} = 2/3$. Such a new 2/3-magnetization plateau was observed in an exact diagonalization study of spatially anisotropic spin-1/2 model¹⁵⁰ but was not seen in more recent variational wave function⁴⁵ and DMRG⁴⁷, as well as in analytical large- S ^{28,50} studies.

Nearly isotropic, $J'/J \approx 1$, antiferromagnet $\text{Ba}_3\text{CoSb}_2\text{O}_9$ is believed to provide an ‘ideal’ realization of the spin-1/2 antiferromagnet on a uniform triangular lattice^{151,152}. And, indeed, its experimental phase diagram is in close correspondence with $J' = J$ ‘cut in Figure 5 (along $\delta = 0$ line) and Figure 7 (along $R = 0$ line): it has 120° spin structure at zero field, coplanar Y state at low fields, the 1/3 magnetization plateau in the $h_{c1}/h_{\text{sat}} = 0.3 \leq h/h_{\text{sat}} \leq h_{c2}/h_{\text{sat}} = 0.47$ interval, and coplanar V state (denoted as 2 : 1 state in¹⁵¹) at higher fields.

A new element of the study^{151,152} is the appearance of weak anomaly in dM/dB at about $M/M_{\text{sat}} = 3/5$, which was interpreted as a quantum phase transition from the V phase to another coplanar phase - inverted Y (state ‘e’ in Figure 2). Near the saturation field these two phases are very close in energy, the difference appears only in the 6th order in condensate amplitude⁵³. Such a transition can be driven by sufficiently strong easy-plane anisotropy¹⁵³ as well as anisotropic DM interaction²⁸.

Perhaps, the more relevant to $\text{Ba}_3\text{CoSb}_2\text{O}_9$ is another possibility - that a transition is driven by the interlayer interaction. Ref. 154 has shown that weak inter-plane antiferromagnetic exchange interaction causes transition from the uniform V phase to the *staggered* V phase. The latter is described by the same Eq.(5) but with a z -dependent phase, $\varphi_z = \tilde{\varphi} + \pi z$ (here, z is the integer coordinate of the triangular layer and $\tilde{\varphi}$ is an overall constant phase), leading to the doubling of the period of the magnetic structure along the direction normal to the layer. It is easy to see that such a state actually gains energy from the antiferromagnetic interlayer exchange J'' , while preserving the optimal in-plane configuration in every layer. Such a transition, denoted as HFC1-HFC2 transition, was also observed in recent semi-classical Monte Carlo simulations¹⁵⁵. This development suggest that a mysterious ‘2/3-plateau’ of Cs_2CuBr_4 , mentioned above, may too

be related to a transition between the lower-field uniform and higher-field staggered versions of the commensurate V phase.

B. SDW and spin nematic phases

A collinear SDW order has been observed in spin-1/2 Ising-like antiferromagnet $\text{BaCo}_2\text{V}_2\text{O}_8$. Experimental confirmations of this comes from specific heat¹⁵⁶ and neutron diffraction¹⁵⁷ measurements. The latter one is particularly important as it proofs the linear scaling of the SDW ordering wave vector with the magnetization, $k_{\text{sdw}} = \pi(1 - 2M)$, predicted in¹⁵⁸. Subsequent NMR¹⁵⁹, ultrasound¹⁶⁰, and neutron scattering¹⁶¹ experiments have refined the phase diagram and even proposed the existence of two different SDW phases¹⁵⁹ stabilized by competing interchain interactions.

Most recently, spin-1/2 magnetic insulator LiCuVO_4 has emerged^{162,163} as a promising candidate to realize both a high-field spin nematic phase, right below the two-magnon saturation field, which is about 45 T high, and an incommensurate collinear SDW phase at lower fields, extending from about 40T down to about 10 T. At yet lower magnetic field, the material realizes more conventional vector chiral (umbrella) state which can be stabilized by a moderate easy-plane anisotropy of exchange interactions¹⁶⁴ (which does not affect the high field physics discussed here).

This last material seems to nicely realize theoretical scenario outlined in Section IV B 1: spin-nematic chains^{165,166} form a two-dimensional nematic phase only in the immediate vicinity of the saturation field¹⁶⁷. At fields below that rather narrow interval, the ground state is an incommensurate longitudinal SDW state. Evidence for the latter includes detailed studies of NMR line shape^{168–171} and neutron scattering^{172,173}. It is worth adding here that quasi-one-dimensional nature of this material is evident from the very pronounced multi-spinon continuum, observed at $h = 0$ in inelastic neutron scattering studies¹⁷⁴.

C. Weak Mott insulators: Hubbard model on anisotropic triangular lattice

Given that, quite generally, Heisenberg Hamiltonian can be viewed as a strong-coupling (large U/t) limit of the Hubbard model, it is natural to consider the fate of the Hubbard $t - t' - U$ model on (spatially anisotropic, in general) triangular lattice.

As a matter of fact, this very problem is of immediate relevance to intriguing experiments on organic Mott insulators of $\text{X}[\text{Pd}(\text{dmit})_2]_2$ and $\kappa\text{-(ET)}_2\text{Z}$ families. Recent experimental^{18,175} and theoretical^{12,176–178} reviews describe key relevant to these materials issues, and we direct interested readers to these publications.

One of the main unresolved issues in this field is that of a proper minimal model that captures all relevant degrees of freedom. Highly successful initial proposal¹⁸¹ models the system as a simple half-filled Hubbard model on a spatially

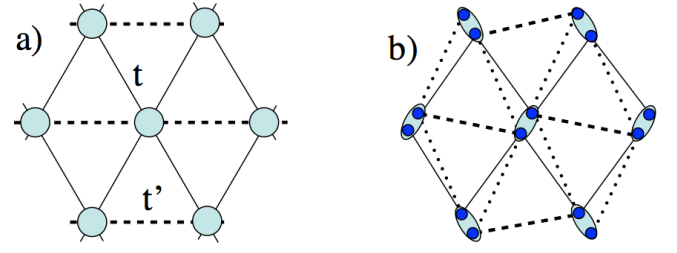


FIG. 12: (a) Spatially anisotropic single-band Hubbard model for organic Mott insulators, after Refs.8,179. Note that $t'/t < 1$ here implies $J/J' < 1$ in Figure 1: J' of Fig. 1 actually lives on t bonds of the Hubbard model here. (b) Geometry of an extended two-band model, after Ref.180. The 'sites', shown by filled dots inside ovals representing dimers, are now two-molecule dimers. Two sites from the same dimer are connected by the intra-dimer tunneling amplitude t_d , and in the limit $t_d \gg$ 'inter-dimer tunnelings' the model reduces to that in (a). Note also the appearance of additional hopping amplitudes (dotted line) connecting 'more distant' sites of neighboring dimers.

anisotropic triangular lattice, as sketched in Figure 12. Every 'site' of this lattice in fact represents closely bound dimer, made of two ET molecules¹⁸¹, and occupied by single electron (or hole). Spatial anisotropy shows up via different hopping integrals t, t' . Within the standard large- U description, anisotropy of hopping t'/t directly translates into that of exchange interactions on different bonds, $J'/J \sim (t'/t)^2$. Ironically, most of the studied materials fall onto $t' < t$ side^{8,179} of the diagram, which happens to be opposite to $J > J'$ limit of spatially anisotropic Heisenberg model, to which this review is devoted.

This description has generated a large number of interesting studies, the full list of which is beyond the scope of this review. One of the main outcomes of these studies is the establishment of approximate $t'/t - U$ phase diagram (see for example Figure 6 of¹⁸²) which harbors metallic phase (for $U/t \lesssim 10$ or less, depending on t'/t) and various insulating magnetic phases, which include both the standard Néel and non-coplanar spiral phases as well as quantum-disordered spin-liquid state (for $t'/t \approx 0.9$ and $U/t \gtrsim 12$).

Thinking in terms of effective spin-only model, it is important to realize that for not too large U/t , the standard Heisenberg model must be amended with *ring-exchange* terms involving four (or more) long spin loops^{183,184}. This addition dramatically affects the regime of intermediate U/t by stabilizing an insulating spin-liquid ground state^{184,185}. The nature of the emerging spin-liquid is subject of intense on-going investigations, with proposals ranging from Z_2 liquid^{186,187} to spin Bose-metal¹⁸⁸, to spin-liquid with quadratic band touching¹⁸⁹.

Recently, however, this appealing spin-only picture of the organic Mott insulators has been challenged by the experimental discovery of anomalous response of dielectric constant¹⁹⁰ and lattice expansion coefficient¹⁹¹ at low temperature. This finding imply that charge degrees of freedom, assumed frozen in the spin-only description, are actually present

in the material and have to be accounted for in theoretical modeling. Several subsequent papers^{180,192,193} have identified dimer units of the triangular lattice, viewed as sites in Figure 12, as the most likely place where charge dynamics persists down to lowest temperatures. To describe these internal states of the two-molecule dimers, one need to go back to a two-band extended Hubbard model description¹⁹⁴. Taking the strong-coupling of such a model, one derives¹⁸⁰ a coupled dynamics of interacting spins and *electric dipoles* on the triangular lattice. It turns out that sufficiently strong inter-dimer Coulomb interaction stabilizes charge-ordered state (dipolar solid) and suppresses spin ordering via non-trivial modification of exchange interactions J, J' .

Clearly many more studies, both experimental and theoretical, are required in order to elucidate the physics behind apparent spin-liquid behavior of organic Mott insulators.

In place of conclusion we just state the obvious: despite many years of investigations, quantum magnets on triangular lattices continue to surprise us. There are no doubts that future studies of new materials and models, inspired by them, will bring out new quantum states and phenomena.

Acknowledgments

I am grateful to my friends and coauthors - Leon Balents, Andrey Chubukov, Jason Alicea and Zhihao Hao - for fruitful

collaborations and countless insightful discussions that provide the foundation of this review. I thank Sasha Abanov, Hosho Katsura, Ru Chen, Hyejin Ju, Hong-Chen Jiang, Christian Griset, and Shane Head for their crucial contributions to joint investigations related to the topics discussed here. Discussions of experiments with Collin Broholm, Radu Coldea, Martin Mourigal, Masashi Takigawa, Leonid Svistov, Alexander Smirnov and Yasu Takano are greatly appreciated as well. I have benefited extensively from conversations with Cristian Batista, Misha Raikh, Dima Pesin, Eugene Mishchenko and Oleg Tchernyhyov. Many thanks to Luis Seabra, Nic Shannon, Alexander Smirnov and Yasu Takano for permissions to reproduce figures from their papers in this review. Special thanks to Andrey Chubukov for the critical reading of the manuscript and invaluable comments. This work is supported by the National Science Foundation through grant DMR-12-06774.

- ¹ Y. Zhang, T. Grover, A. Turner, M. Oshikawa, and A. Vishwanath. ‘Quasiparticle statistics and braiding from ground-state entanglement.’ *Phys. Rev. B*, **85**, 235151 (2012). doi:10.1103/PhysRevB.85.235151.
- ² H.-C. Jiang, Z. Wang, and L. Balents. ‘Identifying topological order by entanglement entropy.’ *Nature Physics*, **8**, 902–905 (2012). doi:10.1038/nphys2465.
- ³ T. Grover, Y. Zhang, and A. Vishwanath. ‘Entanglement entropy as a portal to the physics of quantum spin liquids.’ *New Journal of Physics*, **15**, 025002 (2013).
- ⁴ S. Yan, D. A. Huse, and S. R. White. ‘Spin-Liquid Ground State of the $S = 1/2$ Kagome Heisenberg Antiferromagnet.’ *Science*, **332**, 1173–1176 (2011). doi:10.1126/science.1201080.
- ⁵ H.-C. Jiang, H. Yao, and L. Balents. ‘Spin liquid ground state of the spin- $\frac{1}{2}$ square J_1 - J_2 Heisenberg model.’ *Phys. Rev. B*, **86**, 024424 (2012). doi:10.1103/PhysRevB.86.024424.
- ⁶ S. Depenbrock, I. P. McCulloch, and U. Schollwöck. ‘Nature of the Spin-Liquid Ground State of the $S = 1/2$ Heisenberg Model on the Kagome Lattice.’ *Phys. Rev. Lett.*, **109**, 067201 (2012). doi:10.1103/PhysRevLett.109.067201.
- ⁷ Y. Shimizu, K. Miyagawa, K. Kanoda, M. Maesato, and G. Saito. ‘Spin Liquid State in an Organic Mott Insulator with a Triangular Lattice.’ *Phys. Rev. Lett.*, **91**, 107001 (2003). doi:10.1103/PhysRevLett.91.107001.
- ⁸ K. Kanoda and R. Kato. ‘Mott Physics in Organic Conductors with Triangular Lattices.’ *Annual Review of Condensed Matter Physics*, **2**, 167–188 (2011). doi:10.1146/annurev-conmatphys-062910-140521. <http://www.annualreviews.org/doi/pdf/10.1146/annurev-conmatphys-062910-140521>.
- ⁹ T.-H. Han, J. S. Helton, S. Chu, D. G. Nocera, J. A. Rodriguez-Rivera, C. Broholm, and Y. S. Lee. ‘Fractionalized excitations in the spin-liquid state of a kagome-lattice antiferromagnet.’ *Nature* (London), **492**, 406–410 (2012). doi:10.1038/nature11659.
- ¹⁰ M. F. Collins and O. A. Petrenko. ‘Triangular antiferromagnets.’ *Canadian Journal of Physics*, **75**, 605–655 (1997). doi:10.1139/p97-007. <http://www.nrcresearchpress.com/doi/pdf/10.1139/p97-007>.
- ¹¹ A. Ramirez. ‘“Geometrical frustration”.’ In K. Buschow, editor, ‘Handbook of Magnetic Materials,’ volume 13, chapter 4, pages 423 – 520. Elsevier (2001). doi:http://dx.doi.org/10.1016/S1567-2719(01)13008-8.
- ¹² L. Balents. ‘Spin liquids in frustrated magnets.’ *Nature*, **464**, 199–208 (2010).
- ¹³ G. H. Wannier. ‘Antiferromagnetism. The Triangular Ising Net.’ *Phys. Rev.*, **79**, 357–364 (1950). doi:10.1103/PhysRev.79.357.
- ¹⁴ D. Huse and V. Elser. ‘Simple Variational Wave Functions for Two-Dimensional Heisenberg Spin-1/2 Antiferromagnets.’ *Phys. Rev. Lett.*, **60**, 2531–2534 (1988).
- ¹⁵ B. Bernu, C. Lhuillier, and L. Pierre. ‘Signature of Néel order in exact spectra of quantum antiferromagnets on finite lattices.’ *Phys. Rev. Lett.*, **69**, 2590–2593 (1992). doi:10.1103/PhysRevLett.69.2590.
- ¹⁶ S. R. White and A. L. Chernyshev. ‘Néel Order in Square and Triangular Lattice Heisenberg Models.’ *Phys. Rev. Lett.*, **99**, 127004 (2007). doi:10.1103/PhysRevLett.99.127004.
- ¹⁷ P. Anderson. ‘Resonating valence bonds: a new kind of insulator?’ *Materials Research Bulletin*, **8**, 153–160 (1973).
- ¹⁸ P. Fazekas and P. Anderson. ‘On the ground state properties of the anisotropic triangular antiferromagnet.’ *Philosophical Magazine*,

- 30**, 423–440 (1974).
- ¹⁹ R. Moessner and S. L. Sondhi. ‘Resonating Valence Bond Phase in the Triangular Lattice Quantum Dimer Model.’ *Phys. Rev. Lett.*, **86**, 1881–1884 (2001). doi:10.1103/PhysRevLett.86.1881.
 - ²⁰ P. Mendels and A. Wills. ‘Kagome Antiferromagnets: Materials Vs. Spin Liquid Behaviors.’ In C. Lacroix, P. Mendels, and F. Mila, editors, ‘Introduction to Frustrated Magnetism,’ volume 164 of *Springer Series in Solid-State Sciences*, pages 207–238. Springer Berlin Heidelberg (2011). ISBN 978-3-642-10588-3. doi:10.1007/978-3-642-10589-0.9.
 - ²¹ Z. Nussinov and J. van den Brink. ‘Compass and Kitaev models – Theory and Physical Motivations.’ ArXiv:1303.5922 (2013). 1303.5922.
 - ²² W. Witczak-Krempa, G. Chen, Y. B. Kim, and L. Balents. ‘Correlated Quantum Phenomena in the Strong Spin-Orbit Regime.’ *Annual Review of Condensed Matter Physics*, **5**, 57–82 (2014). doi:10.1146/annurev-conmatphys-020911-125138.
 - ²³ H. Kawamura and S. Miyashita. ‘Phase Transition of the Heisenberg Antiferromagnet on the Triangular Lattice in a Magnetic Field.’ *Journal of the Physical Society of Japan*, **54**, 4530–4538 (1985). doi:10.1143/JPSJ.54.4530.
 - ²⁴ J. Chalker. ‘Geometrically Frustrated Antiferromagnets: Statistical Mechanics and Dynamics.’ In C. Lacroix, P. Mendels, and F. Mila, editors, ‘Introduction to Frustrated Magnetism,’ volume 164 of *Springer Series in Solid-State Sciences*, pages 3–22. Springer Berlin Heidelberg (2011). ISBN 978-3-642-10588-3. doi:10.1007/978-3-642-10589-0.1.
 - ²⁵ L. Seabra, T. Momoi, P. Sindzingre, and N. Shannon. ‘Phase diagram of the classical Heisenberg antiferromagnet on a triangular lattice in an applied magnetic field.’ *Phys. Rev. B*, **84**, 214418 (2011). doi:10.1103/PhysRevB.84.214418.
 - ²⁶ M. V. Gvozdikova, P.-E. Melchy, and M. E. Zhitomirsky. ‘Magnetic phase diagrams of classical triangular and kagome antiferromagnets.’ *Journal of Physics: Condensed Matter*, **23**, 164209 (2011).
 - ²⁷ A. I. Smirnov, H. Yashiro, S. Kimura, M. Hagiwara, Y. Narumi, K. Kindo, A. Kikkawa, K. Katsumata, A. Y. Shapiro, and L. N. Demianets. ‘Triangular lattice antiferromagnet $\text{RbFe}(\text{MoO}_4)_2$ in high magnetic fields.’ *Phys. Rev. B*, **75**, 134412 (2007). doi:10.1103/PhysRevB.75.134412.
 - ²⁸ C. Grisetti, S. Head, J. Alicea, and O. A. Starykh. ‘Deformed triangular lattice antiferromagnets in a magnetic field: Role of spatial anisotropy and Dzyaloshinskii-Moriya interactions.’ *Phys. Rev. B*, **84**, 245108 (2011). doi:10.1103/PhysRevB.84.245108.
 - ²⁹ H. Kawamura and S. Miyashita. ‘Phase Transition of the Two-Dimensional Heisenberg Antiferromagnet on the Triangular Lattice.’ *Journal of the Physical Society of Japan*, **53**, 4138–4154 (1984). doi:10.1143/JPSJ.53.4138.
 - ³⁰ S. E. Korshunov. ‘Phase transitions in two-dimensional systems with continuous degeneracy.’ *Physics-Uspekhi*, **49**, 225 (2006).
 - ³¹ H. Kawamura, A. Yamamoto, and T. Okubo. ‘ Z_2 -Vortex Ordering of the Triangular-Lattice Heisenberg Antiferromagnet.’ *Journal of the Physical Society of Japan*, **79**, 023701 (2010). doi:10.1143/JPSJ.79.023701.
 - ³² M. Wintel, H. U. Everts, and W. Apel. ‘Monte Carlo simulation of the Heisenberg antiferromagnet on a triangular lattice: Topological excitations.’ *Phys. Rev. B*, **52**, 13480–13486 (1995). doi:10.1103/PhysRevB.52.13480.
 - ³³ B. Southern and H.-J. Xu. ‘Monte Carlo study of the Heisenberg antiferromagnet on the triangular lattice.’ *Phys. Rev. B*, **52**, R3836–R3839 (1995). doi:10.1103/PhysRevB.52.R3836.
 - ³⁴ P. Azaria, B. Delamotte, and D. Mouhanna. ‘Low-temperature properties of two-dimensional frustrated quantum antiferromagnets.’ *Phys. Rev. Lett.*, **68**, 1762–1765 (1992). doi:10.1103/PhysRevLett.68.1762.
 - ³⁵ D. Mouhanna, B. Delamotte, J.-P. Kownacki, and M. Tissier. ‘NON-PERTURBATIVE RENORMALIZATION GROUP: BASIC PRINCIPLES AND SOME APPLICATIONS.’ *Modern Physics Letters B*, **25**, 873–889 (2011).
 - ³⁶ N. Hasselmann and A. Sinner. ‘Interplay of topology and geometry in frustrated two-dimensional Heisenberg magnets.’ *Phys. Rev. B*, **90**, 094404 (2014). doi:10.1103/PhysRevB.90.094404.
 - ³⁷ H. Kawamura. ‘ Z_2 -vortex order of frustrated Heisenberg antiferromagnets in two dimensions.’ *Journal of Physics: Conference Series*, **320**, 012002 (2011).
 - ³⁸ C. Pinettes, B. Canals, and C. Lacroix. ‘Classical Heisenberg antiferromagnet away from the pyrochlore lattice limit: Entropic versus energetic selection.’ *Phys. Rev. B*, **66**, 024422 (2002). doi:10.1103/PhysRevB.66.024422.
 - ³⁹ M. Moliner, D. C. Cabra, A. Honecker, P. Pujol, and F. Stauffer. ‘Magnetization process in the classical Heisenberg model on the Shastry-Sutherland lattice.’ *Phys. Rev. B*, **79**, 144401 (2009). doi:10.1103/PhysRevB.79.144401.
 - ⁴⁰ I. Pomeranchuk. ‘On the theory of liquid He 3.’ *Zh. Eksp. Teor. Fiz.*, **20**, 919 (1950).
 - ⁴¹ R. C. Richardson. ‘The Pomeranchuk effect.’ *Rev. Mod. Phys.*, **69**, 683–690 (1997). doi:10.1103/RevModPhys.69.683.
 - ⁴² A. V. Chubukov and D. I. Golosov. ‘Quantum theory of an antiferromagnet on a triangular lattice in a magnetic field.’ *Journal of Physics: Condensed Matter*, **3**, 69 (1991).
 - ⁴³ A. Honecker, J. Schulenburg, and J. Richter. ‘Magnetization plateaus in frustrated antiferromagnetic quantum spin models.’ *Journal of Physics: Condensed Matter*, **16**, S749 (2004).
 - ⁴⁴ D. J. J. Farnell, R. Zinke, J. Schulenburg, and J. Richter. ‘High-order coupled cluster method study of frustrated and unfrustrated quantum magnets in external magnetic fields.’ *Journal of Physics: Condensed Matter*, **21**, 406002 (2009).
 - ⁴⁵ T. Tay and O. I. Motrunich. ‘Variational studies of triangular Heisenberg antiferromagnet in magnetic field.’ *Phys. Rev. B*, **81**, 165116 (2010).
 - ⁴⁶ T. Sakai and H. Nakano. ‘Critical magnetization behavior of the triangular- and kagome-lattice quantum antiferromagnets.’ *Phys. Rev. B*, **83**, 100405 (2011). doi:10.1103/PhysRevB.83.100405.
 - ⁴⁷ R. Chen, H. Ju, H.-C. Jiang, O. A. Starykh, and L. Balents. ‘Ground states of spin- $\frac{1}{2}$ triangular antiferromagnets in a magnetic field.’ *Phys. Rev. B*, **87**, 165123 (2013). doi:10.1103/PhysRevB.87.165123.
 - ⁴⁸ C. Hotta, S. Nishimoto, and N. Shibata. ‘Grand canonical finite size numerical approaches in one and two dimensions: Real space energy renormalization and edge state generation.’ *Phys. Rev. B*, **87**, 115128 (2013). doi:10.1103/PhysRevB.87.115128.
 - ⁴⁹ G. Murthy, D. Arovas, and A. Auerbach. ‘Superfluids and super-solids on frustrated two-dimensional lattices.’ *Phys. Rev. B*, **55**, 3104–3121 (1997). doi:10.1103/PhysRevB.55.3104.
 - ⁵⁰ J. Alicea, A. V. Chubukov, and O. A. Starykh. ‘Quantum Stabilization of the $1/3$ -Magnetization Plateau in $\text{Cs}_{-2}\text{CuBr}_{-4}$.’ *Phys. Rev. Lett.*, **102**, 137201 (2009).
 - ⁵¹ A. V. Chubukov and O. A. Starykh. ‘Spin-Current Order in Anisotropic Triangular Antiferromagnets.’ *Phys. Rev. Lett.*, **110**, 217210 (2013). doi:10.1103/PhysRevLett.110.217210.
 - ⁵² O. A. Starykh, W. Jin, and A. V. Chubukov. ‘Phases of a Triangular-Lattice Antiferromagnet Near Saturation.’ *Phys. Rev. Lett.*, **113**, 087204 (2014). doi:10.1103/PhysRevLett.113.087204.
 - ⁵³ T. Nikuni and H. Shiba. ‘Hexagonal antiferromagnets in strong magnetic field: mapping onto Bose condensation of low-density Bose gas.’ *Journal of the Physical Society of Japan*, **64**, 3471–3483 (1995).

- ⁵⁴ Z. Weihong, R. H. McKenzie, and R. R. P. Singh. 'Phase diagram for a class of spin- $\frac{1}{2}$ Heisenberg models interpolating between the square-lattice, the triangular-lattice, and the linear-chain limits.' *Phys. Rev. B*, **59**, 14367–14375 (1999). doi:10.1103/PhysRevB.59.14367.
- ⁵⁵ O. A. Starykh, A. V. Chubukov, and A. G. Abanov. 'Flat spin-wave dispersion in a triangular antiferromagnet.' *Phys. Rev. B*, **74**, 180403 (2006). doi:10.1103/PhysRevB.74.180403.
- ⁵⁶ A. L. Chernyshev and M. E. Zhitomirsky. 'Magnon Decay in Noncollinear Quantum Antiferromagnets.' *Phys. Rev. Lett.*, **97**, 207202 (2006). doi:10.1103/PhysRevLett.97.207202.
- ⁵⁷ M. E. Zhitomirsky and A. L. Chernyshev. 'Spontaneous magnon decays.' *Rev. Mod. Phys.*, **85**, 219–242 (2013). doi:10.1103/RevModPhys.85.219.
- ⁵⁸ W. Zheng, J. O. Fjærestad, R. R. P. Singh, R. H. McKenzie, and R. Coldea. 'Excitation spectra of the spin- $\frac{1}{2}$ triangular-lattice Heisenberg antiferromagnet.' *Phys. Rev. B*, **74**, 224420 (2006). doi:10.1103/PhysRevB.74.224420.
- ⁵⁹ A. Mezio, L. O. Manuel, R. R. P. Singh, and A. E. Trumper. 'Low temperature properties of the triangular-lattice antiferromagnet: a bosonic spinon theory.' *New Journal of Physics*, **14**, 123033 (2012).
- ⁶⁰ A. Weichselbaum and S. R. White. 'Incommensurate correlations in the anisotropic triangular Heisenberg lattice.' *Phys. Rev. B*, **84**, 245130 (2011). doi:10.1103/PhysRevB.84.245130.
- ⁶¹ D. Heidarian, S. Sorella, and F. Becca. 'Spin-1/2 Heisenberg model on the anisotropic triangular lattice: From magnetism to a one-dimensional spin liquid.' *Phys. Rev. B*, **80**, 012404 (2009).
- ⁶² M. Weng, D. Sheng, Z. Weng, and R. Bursill. 'Spin-liquid phase in an anisotropic triangular-lattice Heisenberg model: Exact diagonalization and density-matrix renormalization group calculations.' *Phys. Rev. B*, **74**, 012407 (2006).
- ⁶³ T. Pardini and R. Singh. 'Magnetic order in coupled spin-half and spin-one Heisenberg chains in an anisotropic triangular-lattice geometry.' *Phys. Rev. B*, **77**, 214433 (2008).
- ⁶⁴ O. A. Starykh and L. Balents. 'Ordering in spatially anisotropic triangular antiferromagnets.' *Phys. Rev. Lett.*, **98**, 77205 (2007).
- ⁶⁵ R. F. Bishop, P. H. Y. Li, D. J. J. Farnell, and C. E. Campbell. 'Magnetic order in a spin- $\frac{1}{2}$ interpolating square-triangle Heisenberg antiferromagnet.' *Phys. Rev. B*, **79**, 174405 (2009). doi:10.1103/PhysRevB.79.174405.
- ⁶⁶ R. F. Bishop, P. H. Y. Li, D. J. J. Farnell, and C. E. Campbell. 'MAGNETIC ORDERING OF ANTIFERROMAGNETS ON A SPATIALLY ANISOTROPIC TRIANGULAR LATTICE.' *International Journal of Modern Physics B*, **24**, 5011–5026 (2010). doi:10.1142/S021797921005716X. <http://www.worldscientific.com/doi/pdf/10.1142/S021797921005716X>.
- ⁶⁷ J. Reuther and R. Thomale. 'Functional renormalization group for the anisotropic triangular antiferromagnet.' *Phys. Rev. B*, **83**, 024402 (2011). doi:10.1103/PhysRevB.83.024402.
- ⁶⁸ S. Ghamari, C. Kallin, S.-S. Lee, and E. S. Sørensen. 'Order in a spatially anisotropic triangular antiferromagnet.' *Phys. Rev. B*, **84**, 174415 (2011). doi:10.1103/PhysRevB.84.174415.
- ⁶⁹ O. A. Starykh, H. Katsura, and L. Balents. 'Extreme sensitivity of a frustrated quantum magnet: Cs_2CuCl_4 .' *Phys. Rev. B*, **82**, 014421 (2010).
- ⁷⁰ G. Grüner. 'The dynamics of charge-density waves.' *Rev. Mod. Phys.*, **60**, 1129–1181 (1988). doi:10.1103/RevModPhys.60.1129.
- ⁷¹ G. Grüner. 'The dynamics of spin-density waves.' *Rev. Mod. Phys.*, **66**, 1–24 (1994). doi:10.1103/RevModPhys.66.1.
- ⁷² P. Monceau. 'Electronic crystals: an experimental overview.' *Advances in Physics*, **61**, 325–581 (2012). doi:10.1080/00018732.2012.719674.
- ⁷³ I. Affleck. 'Field Theory Methods and Quantum Critical Phenomena.' In E. Brézin and J. Zinn-Justin, editors, 'Fields, Strings and Critical Phenomena,' pages 563–640. North-Holland, Amsterdam (1988).
- ⁷⁴ A. O. Gogolin, A. A. Nersisyan, and A. M. Tsvelik. *Bosonization and strongly correlated systems*. Cambridge University Press (2004).
- ⁷⁵ O. A. Starykh, A. Furusaki, and L. Balents. 'Anisotropic pyrochlores and the global phase diagram of the checkerboard antiferromagnet.' *Phys. Rev. B*, **72**, 094416 (2005).
- ⁷⁶ O. A. Starykh and L. Balents. 'Excitations and quasi-one-dimensionality in field-induced nematic and spin density wave states.' *Phys. Rev. B*, **89**, 104407 (2014). doi:10.1103/PhysRevB.89.104407.
- ⁷⁷ I. Affleck and G. F. Wellman. 'Longitudinal modes in quasi-one-dimensional antiferromagnets.' *Phys. Rev. B*, **46**, 8934–8953 (1992). doi:10.1103/PhysRevB.46.8934.
- ⁷⁸ H. J. Schulz. 'Dynamics of Coupled Quantum Spin Chains.' *Phys. Rev. Lett.*, **77**, 2790–2793 (1996). doi:10.1103/PhysRevLett.77.2790.
- ⁷⁹ J. A. Blanco, B. Fåk, J. Jensen, M. Rotter, A. Hiess, D. Schmitt, and P. Lejay. 'Phasons, amplitude modes, and spin waves in the amplitude-modulated magnetic phase of PrNi_2Si_2 .' *Phys. Rev. B*, **87**, 104411 (2013). doi:10.1103/PhysRevB.87.104411.
- ⁸⁰ K. Okunishi and T. Suzuki. 'Field-induced incommensurate order for the quasi-one-dimensional XXZ model in a magnetic field.' *Phys. Rev. B*, **76**, 224411 (2007). doi:10.1103/PhysRevB.76.224411.
- ⁸¹ I. Affleck. 'Theory of Haldane-gap antiferromagnets in applied fields.' *Phys. Rev. B*, **41**, 6697–6702 (1990). doi:10.1103/PhysRevB.41.6697.
- ⁸² S. Sachdev, T. Senthil, and R. Shankar. 'Finite-temperature properties of quantum antiferromagnets in a uniform magnetic field in one and two dimensions.' *Phys. Rev. B*, **50**, 258–272 (1994). doi:10.1103/PhysRevB.50.258.
- ⁸³ A. Zheludev, Z. Honda, Y. Chen, C. L. Broholm, K. Katsumata, and S. M. Shapiro. 'Quasielastic Neutron Scattering in the High-Field Phase of a Haldane Antiferromagnet.' *Phys. Rev. Lett.*, **88**, 077206 (2002). doi:10.1103/PhysRevLett.88.077206.
- ⁸⁴ F. H. L. Essler and I. Affleck. 'Haldane-gap chains in a magnetic field.' *Journal of Statistical Mechanics: Theory and Experiment*, **2004**, P12006 (2004).
- ⁸⁵ R. M. Konik and P. Fendley. 'Haldane-gapped spin chains as Luttinger liquids: Correlation functions at finite field.' *Phys. Rev. B*, **66**, 144416 (2002). doi:10.1103/PhysRevB.66.144416.
- ⁸⁶ G. Fáth. 'Luttinger liquid behavior in spin chains with a magnetic field.' *Phys. Rev. B*, **68**, 134445 (2003). doi:10.1103/PhysRevB.68.134445.
- ⁸⁷ I. P. McCulloch, R. Kube, M. Kurz, A. Kleine, U. Schollwöck, and A. K. Kolezhuk. 'Vector chiral order in frustrated spin chains.' *Phys. Rev. B*, **77**, 094404 (2008). doi:10.1103/PhysRevB.77.094404.
- ⁸⁸ M. Oshikawa, M. Yamanaka, and I. Affleck. 'Magnetization Plateaus in Spin Chains: "Haldane Gap" for Half-Integer Spins.' *Phys. Rev. Lett.*, **78**, 1984–1987 (1997). doi:10.1103/PhysRevLett.78.1984.
- ⁸⁹ M. Oshikawa. 'Insulator, Conductor, and Commensurability: A Topological Approach.' *Phys. Rev. Lett.*, **90**, 236401 (2003). doi:10.1103/PhysRevLett.90.236401.
- ⁹⁰ K. Okunishi and T. Tonegawa. 'Magnetic Phase Diagram of the $S = 1/2$ Antiferromagnetic Zigzag Spin Chain in the Strongly Frustrated Region: Cusp and Plateau.' *Journal of the Physical Society of Japan*, **72**, 479–482 (2003). doi:10.1143/JPSJ.72.479.

- ⁹¹ F. Heidrich-Meisner, I. A. Sergienko, A. E. Feiguin, and E. R. Dagotto. ‘Universal emergence of the one-third plateau in the magnetization process of frustrated quantum spin chains.’ *Phys. Rev. B*, **75**, 064413 (2007). doi:10.1103/PhysRevB.75.064413.
- ⁹² T. Hikihara, T. Momoi, A. Furusaki, and H. Kawamura. ‘Magnetic phase diagram of the spin- $\frac{1}{2}$ antiferromagnetic zigzag ladder.’ *Phys. Rev. B*, **81**, 224433 (2010). doi:10.1103/PhysRevB.81.224433.
- ⁹³ A. F. Andreev and I. A. Grishchuk. ‘Spin nematics.’ *JETP*, **60**, 267 (1984).
- ⁹⁴ P. Chandra and P. Coleman. ‘Quantum spin nematics: Moment-free magnetism.’ *Phys. Rev. Lett.*, **66**, 100–103 (1991). doi:10.1103/PhysRevLett.66.100.
- ⁹⁵ A. V. Chubukov. ‘Chiral, nematic, and dimer states in quantum spin chains.’ *Phys. Rev. B*, **44**, 4693–4696 (1991). doi:10.1103/PhysRevB.44.4693.
- ⁹⁶ T. Hikihara, L. Kecke, T. Momoi, and A. Furusaki. ‘Vector chiral and multipolar orders in the spin- $\frac{1}{2}$ frustrated ferromagnetic chain in magnetic field.’ *Phys. Rev. B*, **78**, 144404 (2008). doi:10.1103/PhysRevB.78.144404.
- ⁹⁷ M. Blume and Y. Y. Hsieh. ‘Biquadratic Exchange and Quadrupolar Ordering.’ *Journal of Applied P*, **40**, 1249 (1969).
- ⁹⁸ P. Chandra, P. Coleman, and A. I. Larkin. ‘A quantum fluids approach to frustrated Heisenberg models.’ *Journal of Physics: Condensed Matter*, **2**, 7933 (1990).
- ⁹⁹ M. E. Zhitomirsky and H. Tsunetsugu. ‘Magnon pairing in quantum spin nematic.’ *EPL (Europhysics Letters)*, **92**, 37001 (2010).
- ¹⁰⁰ M. Sato, T. Hikihara, and T. Momoi. ‘Spin-Nematic and Spin-Density-Wave Orders in Spatially Anisotropic Frustrated Magnets in a Magnetic Field.’ *Phys. Rev. Lett.*, **110**, 077206 (2013). doi:10.1103/PhysRevLett.110.077206.
- ¹⁰¹ A. Jaefari, S. Lal, and E. Fradkin. ‘Charge-density wave and superconductor competition in stripe phases of high-temperature superconductors.’ *Phys. Rev. B*, **82**, 144531 (2010). doi:10.1103/PhysRevB.82.144531.
- ¹⁰² M. P. Zaletel, S. A. Parameswaran, A. Rüegg, and E. Altman. ‘Chiral bosonic Mott insulator on the frustrated triangular lattice.’ *Phys. Rev. B*, **89**, 155142 (2014). doi:10.1103/PhysRevB.89.155142.
- ¹⁰³ A. Dhar, M. Maji, T. Mishra, R. V. Pai, S. Mukerjee, and A. Paramekanti. ‘Bose-Hubbard model in a strong effective magnetic field: Emergence of a chiral Mott insulator ground state.’ *Phys. Rev. A*, **85**, 041602 (2012). doi:10.1103/PhysRevA.85.041602.
- ¹⁰⁴ A. Dhar, T. Mishra, M. Maji, R. V. Pai, S. Mukerjee, and A. Paramekanti. ‘Chiral Mott insulator with staggered loop currents in the fully frustrated Bose-Hubbard model.’ *Phys. Rev. B*, **87**, 174501 (2013). doi:10.1103/PhysRevB.87.174501.
- ¹⁰⁵ G. Misguich, T. Jolicoeur, and S. M. Girvin. ‘Magnetization Plateaus of $\text{SrCu}_2(\text{BO}_3)_2$ from a Chern-Simons Theory.’ *Phys. Rev. Lett.*, **87**, 097203 (2001). doi:10.1103/PhysRevLett.87.097203.
- ¹⁰⁶ K. Hida and I. Affleck. ‘Quantum vs Classical Magnetization Plateaus of $S = 1/2$ Frustrated Heisenberg Chains.’ *Journal of the Physical Society of Japan*, **74**, 1849–1857 (2005). doi:10.1143/JPSJ.74.1849.
- ¹⁰⁷ J. Alicea and M. P. A. Fisher. ‘Critical spin liquid at $\frac{1}{3}$ magnetization in a spin- $\frac{1}{2}$ triangular antiferromagnet.’ *Phys. Rev. B*, **75**, 144411 (2007). doi:10.1103/PhysRevB.75.144411.
- ¹⁰⁸ A. Tanaka, K. Totsuka, and X. Hu. ‘Geometric phases and the magnetization process in quantum antiferromagnets.’ *Phys. Rev. B*, **79**, 064412 (2009). doi:10.1103/PhysRevB.79.064412.
- ¹⁰⁹ M. Takigawa and F. Mila. ‘Magnetization Plateaus.’ In C. Lacroix, P. Mendels, and F. Mila, editors, ‘Introduction to Frustrated Magnetism,’ volume 164 of *Springer Series in Solid-State Sciences*, pages 241–267. Springer Berlin Heidelberg (2011). ISBN 978-3-642-10588-3. doi:10.1007/978-3-642-10589-0_10.
- ¹¹⁰ S. A. Parameswaran, I. Kimchi, A. M. Turner, D. M. Stamper-Kurn, and A. Vishwanath. ‘Wannier Permanent Wave Functions for Featureless Bosonic Mott Insulators on the $1/3$ -Filled Kagome Lattice.’ *Phys. Rev. Lett.*, **110**, 125301 (2013). doi:10.1103/PhysRevLett.110.125301.
- ¹¹¹ S. Nishimoto, N. Shibata, and C. Hotta. ‘Controlling frustrated liquids and solids with an applied field in a kagome Heisenberg antiferromagnet.’ *Nature Communications*, **4**, 2287 (2013). doi:10.1038/ncomms3287.
- ¹¹² S. Capponi, O. Derzhko, A. Honecker, A. M. Läuchli, and J. Richter. ‘Numerical study of magnetization plateaus in the spin- $\frac{1}{2}$ kagome Heisenberg antiferromagnet.’ *Phys. Rev. B*, **88**, 144416 (2013). doi:10.1103/PhysRevB.88.144416.
- ¹¹³ M. E. Zhitomirsky. ‘Field-Induced Transitions in a Kagomé Antiferromagnet.’ *Phys. Rev. Lett.*, **88**, 057204 (2002). doi:10.1103/PhysRevLett.88.057204.
- ¹¹⁴ Z. Hao and O. A. Starykh. ‘Half-metallic magnetization plateaus.’ *Phys. Rev. B*, **87**, 161109 (2013). doi:10.1103/PhysRevB.87.161109.
- ¹¹⁵ I. Martin and C. D. Batista. ‘Itinerant Electron-Driven Chiral Magnetic Ordering and Spontaneous Quantum Hall Effect in Triangular Lattice Models.’ *Physical Review Letters*, **101**, 156402 (2008). doi:10.1103/PhysRevLett.101.156402.
- ¹¹⁶ M. I. Katsnelson, V. Y. Irkhin, L. Chioncel, A. I. Lichtenstein, and R. A. de Groot. ‘Half-metallic ferromagnets: From band structure to many-body effects.’ *Reviews of Modern Physics*, **80**, 315–378 (2008). doi:10.1103/RevModPhys.80.315. 0711.0872.
- ¹¹⁷ R. Nandkishore, L. S. Levitov, and A. V. Chubukov. ‘Chiral superconductivity from repulsive interactions in doped graphene.’ *Nature Physics*, **8**, 158–163 (2012). doi:10.1038/nphys2208.
- ¹¹⁸ R. Nandkishore, G.-W. Chern, and A. V. Chubukov. ‘Itinerant Half-Metal Spin-Density-Wave State on the Hexagonal Lattice.’ *Physical Review Letters*, **108**, 227204 (2012). doi:10.1103/PhysRevLett.108.227204.
- ¹¹⁹ M. L. Kiesel, C. Platt, W. Hanke, D. A. Abanin, and R. Thomale. ‘Competing many-body instabilities and unconventional superconductivity in graphene.’ *Phys. Rev. B*, **86**, 020507 (2012). doi:10.1103/PhysRevB.86.020507. 1109.2953.
- ¹²⁰ G.-W. Chern and C. D. Batista. ‘Spontaneous Quantum Hall Effect via a Thermally Induced Quadratic Fermi Point.’ *Physical Review Letters*, **109**, 156801 (2012). doi:10.1103/PhysRevLett.109.156801.
- ¹²¹ M. W. Zwierlein, A. Schirotzek, C. H. Schunck, and W. Ketterle. ‘Fermionic Superfluidity with Imbalanced Spin Populations.’ *Science*, **311**, 492–496 (2006). doi:10.1126/science.1122318. cond-mat/0511197.
- ¹²² C. Platt, W. Hanke, and R. Thomale. ‘Functional renormalization group for multi-orbital Fermi surface instabilities.’ *Advances in Physics*, **62**, 453–562 (2013). doi:10.1080/00018732.2013.862020.
- ¹²³ R. Coldea, D. A. Tennant, A. M. Tsvelik, and Z. Tylczynski. ‘Experimental Realization of a 2D Fractional Quantum Spin Liquid.’ *Phys. Rev. Lett.*, **86**, 1335–1338 (2001). doi:10.1103/PhysRevLett.86.1335.
- ¹²⁴ R. Coldea, D. A. Tennant, K. Habicht, P. Smeibidl, C. Wolters, and Z. Tylczynski. ‘Direct Measurement of the Spin Hamiltonian and Observation of Condensation of Magnons in the 2D Frustrated Quantum Magnet Cs_2CuCl_4 .’ *Phys. Rev. Lett.*, **88**, 137203 (2002). doi:10.1103/PhysRevLett.88.137203.

- ¹²⁵ R. Coldea, D. A. Tennant, and Z. Tylczynski. ‘Extended scattering continua characteristic of spin fractionalization in the two-dimensional frustrated quantum magnet Cs_2CuCl_4 observed by neutron scattering.’ *Phys. Rev. B*, **68**, 134424 (2003). doi: 10.1103/PhysRevB.68.134424.
- ¹²⁶ M.-A. Vachon, G. Koutroulakis, V. F. Mitrovi, O. Ma, J. B. Marston, A. P. Reyes, P. Kuhns, R. Coldea, and Z. Tylczynski. ‘The nature of the low-energy excitations in the short-range-ordered region of Cs_2CuCl_4 as revealed by ^{133}Cs nuclear magnetic resonance.’ *New Journal of Physics*, **13**, 093029 (2011).
- ¹²⁷ K. Y. Povarov, A. I. Smirnov, O. A. Starykh, S. V. Petrov, and A. Y. Shapiro. ‘Modes of Magnetic Resonance in the Spin-Liquid Phase of Cs_2CuCl_4 .’ *Phys. Rev. Lett.*, **107**, 037204 (2011). doi: 10.1103/PhysRevLett.107.037204.
- ¹²⁸ A. I. Smirnov, K. Y. Povarov, S. V. Petrov, and A. Y. Shapiro. ‘Magnetic resonance in the ordered phases of the two-dimensional frustrated quantum magnet Cs_2CuCl_4 .’ *Phys. Rev. B*, **85**, 184423 (2012). doi:10.1103/PhysRevB.85.184423.
- ¹²⁹ S. A. Zvyagin, M. Ozerov, D. Kamenskyi, J. Wosnitzer, M. Ikeda, T. Fujita, M. Hagiwara, J. Krzystek, R. Hu, H. Ryu, and C. Petrovic. ‘Unconventional spin dynamics in the spin-1/2 triangular-lattice antiferromagnet Cs_2CuBr_4 .’ *ArXiv:1306.3887* (2013). 1306.3887.
- ¹³⁰ M. A. Fayzullin, R. M. Eremina, M. V. Eremin, A. Dittl, N. van Well, F. Ritter, W. Assmus, J. Deisenhofer, H.-A. K. von Nidda, and A. Loidl. ‘Spin correlations and Dzyaloshinskii-Moriya interaction in Cs_2CuCl_4 .’ *Phys. Rev. B*, **88**, 174421 (2013). doi: 10.1103/PhysRevB.88.174421.
- ¹³¹ M. Bocquet, F. H. L. Essler, A. M. Tsvelik, and A. O. Gogolin. ‘Finite-temperature dynamical magnetic susceptibility of quasi-one-dimensional frustrated spin- $\frac{1}{2}$ Heisenberg antiferromagnets.’ *Phys. Rev. B*, **64**, 094425 (2001). doi:10.1103/PhysRevB.64.094425.
- ¹³² J. Alicea, O. I. Motrunich, and M. P. A. Fisher. ‘Algebraic Vortex Liquid in Spin-1/2 Triangular Antiferromagnets: Scenario for Cs_2CuCl_4 .’ *Phys. Rev. Lett.*, **95**, 247203 (2005). doi:10.1103/PhysRevLett.95.247203.
- ¹³³ S. V. Isakov, T. Senthil, and Y. B. Kim. ‘Ordering in Cs_2CuCl_4 : Possibility of a proximate spin liquid.’ *Phys. Rev. B*, **72**, 174417 (2005). doi:10.1103/PhysRevB.72.174417.
- ¹³⁴ M. Y. Veillelte, A. J. A. James, and F. H. L. Essler. ‘Spin dynamics of the quasi-two-dimensional spin- $\frac{1}{2}$ quantum magnet Cs_2CuCl_4 .’ *Phys. Rev. B*, **72**, 134429 (2005). doi:10.1103/PhysRevB.72.134429.
- ¹³⁵ M. Y. Veillelte, J. T. Chalker, and R. Coldea. ‘Ground states of a frustrated spin- $\frac{1}{2}$ antiferromagnet: Cs_2CuCl_4 in a magnetic field.’ *Phys. Rev. B*, **71**, 214426 (2005). doi:10.1103/PhysRevB.71.214426.
- ¹³⁶ W. Zheng, J. O. Fjærestad, R. R. P. Singh, R. H. McKenzie, and R. Coldea. ‘Anomalous Excitation Spectra of Frustrated Quantum Antiferromagnets.’ *Phys. Rev. Lett.*, **96**, 057201 (2006). doi: 10.1103/PhysRevLett.96.057201.
- ¹³⁷ D. Dalidovich, R. Sknepnek, A. J. Berlinsky, J. Zhang, and C. Kallin. ‘Spin structure factor of the frustrated quantum magnet Cs_2CuCl_4 .’ *Phys. Rev. B*, **73**, 184403 (2006). doi: 10.1103/PhysRevB.73.184403.
- ¹³⁸ M. Kohno, O. A. Starykh, and L. Balents. ‘Spinons and triplons in spatially anisotropic frustrated antiferromagnets.’ *Nature Physics*, **3**, 790–795 (2007).
- ¹³⁹ Y. Tokiwa, T. Radu, R. Coldea, H. Wilhelm, Z. Tylczynski, and F. Steglich. ‘Magnetic phase transitions in the two-dimensional frustrated quantum antiferromagnet Cs_2CuCl_4 .’ *Phys. Rev. B*, **73**, 134414 (2006). doi:10.1103/PhysRevB.73.134414.
- ¹⁴⁰ T. Ono, H. Tanaka, H. Aruga Katori, F. Ishikawa, H. Mitamura, and T. Goto. ‘Magnetization plateau in the frustrated quantum spin system Cs_2CuBr_4 .’ *Phys. Rev. B*, **67**, 104431 (2003). doi: 10.1103/PhysRevB.67.104431.
- ¹⁴¹ T. Ono, H. Tanaka, O. Kolomiyets, H. Mitamura, T. Goto, K. Nakajima, A. Oosawa, Y. Koike, K. Kakurai, J. Klenke, P. Smeibidle, and M. Meiner. ‘Magnetization plateaux of the $S = 1/2$ two-dimensional frustrated antiferromagnet Cs_2CuBr_4 .’ *Journal of Physics: Condensed Matter*, **16**, S773 (2004).
- ¹⁴² T. Ono, H. Tanaka, O. Kolomiyets, H. Mitamura, F. Ishikawa, T. Goto, K. Nakajima, A. Oosawa, Y. Koike, K. Kakurai, J. Klenke, P. Smeibidle, M. Meißner, R. Coldea, A. D. Tennant, and J. Ollivier. ‘Field-Induced Phase Transitions Driven by Quantum Fluctuation in $S = 1/2$ Anisotropic Triangular Antiferromagnet Cs_2CuBr_4 .’ *Progress of Theoretical Physics Supplement*, **159**, 217–221 (2005). doi:10.1143/PTPS.159.217.
- ¹⁴³ H. Tsujii, C. R. Rotundu, T. Ono, H. Tanaka, B. Andraka, K. Ingersent, and Y. Takano. ‘Thermodynamics of the up-up-down phase of the $S = \frac{1}{2}$ triangular-lattice antiferromagnet Cs_2CuBr_4 .’ *Phys. Rev. B*, **76**, 060406 (2007). doi:10.1103/PhysRevB.76.060406.
- ¹⁴⁴ L. E. Svistov, A. I. Smirnov, L. A. Prozorova, O. A. Petrenko, A. Micheler, N. Büttgen, A. Y. Shapiro, and L. N. Demianets. ‘Magnetic phase diagram, critical behavior, and two-dimensional to three-dimensional crossover in the triangular lattice antiferromagnet $\text{RbFe}(\text{MoO}_4)_2$.’ *Phys. Rev. B*, **74**, 024412 (2006). doi: 10.1103/PhysRevB.74.024412.
- ¹⁴⁵ J. S. White, C. Niedermayer, G. Gasparovic, C. Broholm, J. M. S. Park, A. Y. Shapiro, L. A. Demianets, and M. Kenzelmann. ‘Multiferroicity in the generic easy-plane triangular lattice antiferromagnet $\text{RbFe}(\text{MoO}_4)_2$.’ *Phys. Rev. B*, **88**, 060409 (2013). doi: 10.1103/PhysRevB.88.060409.
- ¹⁴⁶ Y. Fujii, T. Nakamura, H. Kikuchi, M. Chiba, T. Goto, S. Matsumura, K. Kodama, and M. Takigawa. ‘{NMR} study of $S=12$ quasi-two-dimensional antiferromagnet Cs_2CuBr_4 .’ *Physica B: Condensed Matter*, **346347**, 45 – 49 (2004). ISSN 0921-4526. doi:http://dx.doi.org/10.1016/j.physb.2004.01.017. jce:title;Proceedings of the 7th International Symposium on Research in High Magnetic Fields; jce:title;.
- ¹⁴⁷ Y. Fujii, H. Hashimoto, Y. Yasuda, H. Kikuchi, M. Chiba, S. Matsumura, and M. Takigawa. ‘Commensurate and incommensurate phases of the distorted triangular antiferromagnet Cs_2CuBr_4 studied using ^{133}Cs NMR.’ *Journal of Physics: Condensed Matter*, **19**, 145237 (2007).
- ¹⁴⁸ N. A. Fortune, S. T. Hannahs, Y. Yoshida, T. E. Sherline, T. Ono, H. Tanaka, and Y. Takano. ‘Cascade of Magnetic-Field-Induced Quantum Phase Transitions in a Spin- $\frac{1}{2}$ Triangular-Lattice Antiferromagnet.’ *Phys. Rev. Lett.*, **102**, 257201 (2009). doi: 10.1103/PhysRevLett.102.257201.
- ¹⁴⁹ T. Ono, H. Tanaka, Y. Shirata, A. Matsuo, K. Kindo, F. Ishikawa, O. Kolomiyets, H. Mitamura, T. Goto, H. Nakano, N. A. Fortune, S. T. Hannahs, Y. Yoshida, and Y. Takano. ‘Magnetic-Field Induced Quantum Phase Transitions in Triangular-Lattice Antiferromagnets.’ *Journal of Physics: Conference Series*, **302**, 012003 (2011).
- ¹⁵⁰ S. Miyahara, K. Ogino, and N. Furukawa. ‘Magnetization plateaux of Cs_2CuBr_4 .’ *Physica B: Condensed Matter*, **378380**, 587 – 588 (2006). ISSN 0921-4526. doi:http://dx.doi.org/10.1016/j.physb.2006.01.347. jce:title;Proceedings of the International Conference on Strongly Correlated Electron Systems; jce:subtitle;SCES 2005; jce:subtitle; jxocs:full-name;Proceedings of the International Conference on Strongly Correlated Electron Systems; jxocs:full-name;.
- ¹⁵¹ T. Susuki, N. Kurita, T. Tanaka, H. Nojiri, A. Matsuo, K. Kindo, and H. Tanaka. ‘Magnetization Process and Collective Excita-

- tions in the $S=1/2$ Triangular-Lattice Heisenberg Antiferromagnet $\text{Ba}_3\text{CoSb}_2\text{O}_9$.' *Phys. Rev. Lett.*, **110**, 267201 (2013). doi:10.1103/PhysRevLett.110.267201.
- ¹⁵² Y. Shirata, H. Tanaka, A. Matsuo, and K. Kindo. 'Experimental Realization of a Spin-1/2 Triangular-Lattice Heisenberg Antiferromagnet.' *Phys. Rev. Lett.*, **108**, 057205 (2012). doi:10.1103/PhysRevLett.108.057205.
- ¹⁵³ D. Yamamoto, G. Marmorini, and I. Danshita. 'Quantum Phase Diagram of the Triangular-Lattice XXZ Model in a Magnetic Field.' *Phys. Rev. Lett.*, **112**, 127203 (2014). doi:10.1103/PhysRevLett.112.127203.
- ¹⁵⁴ R. S. Gekht and I. N. Bondarenko. 'Triangular antiferromagnets with a layered structure in a uniform field.' *JETP*, **84**, 345 (1997).
- ¹⁵⁵ G. Koutroulakis, T. Zhou, C. D. Batista, Y. Kamiya, J. D. Thompson, S. E. Brown, and H. D. Zhou. 'Quantum phase diagram of the $S=1/2$ triangular-lattice antiferromagnet $\text{Ba}_3\text{CoSb}_2\text{O}_9$.' *ArXiv:1308.6331* (2013). 1308.6331.
- ¹⁵⁶ S. Kimura, T. Takeuchi, K. Okunishi, M. Hagiwara, Z. He, K. Kindo, T. Taniyama, and M. Itoh. 'Novel Ordering of an $S = 1/2$ Quasi-1D Ising-Like Antiferromagnet in Magnetic Field.' *Phys. Rev. Lett.*, **100**, 057202 (2008). doi:10.1103/PhysRevLett.100.057202.
- ¹⁵⁷ S. Kimura, M. Matsuda, T. Masuda, S. Hondo, K. Kaneko, N. Metoki, M. Hagiwara, T. Takeuchi, K. Okunishi, Z. He, K. Kindo, T. Taniyama, and M. Itoh. 'Longitudinal Spin Density Wave Order in a Quasi-1D Ising-like Quantum Antiferromagnet.' *Phys. Rev. Lett.*, **101**, 207201 (2008). doi:10.1103/PhysRevLett.101.207201.
- ¹⁵⁸ T. Suzuki, N. Kawashima, and K. Okunishi. 'Exotic Finite-Temperature Phase Diagram for Weakly Coupled $S = 1/2$ XXZ Chain in a Magnetic Field.' *Journal of the Physical Society of Japan*, **76**, 123707 (2007). doi:10.1143/JPSJ.76.123707.
- ¹⁵⁹ M. Klanjšek, M. Horvatic, C. Berthier, H. Mayaffre, E. Canevet, B. Grenier, P. Lejay, and E. Orignac. 'Spin-chain system as a tunable simulator of frustrated planar magnetism.' *ArXiv:1202.6374* (2012). 1202.6374.
- ¹⁶⁰ H. Yamaguchi, S. Yasin, S. Zherlitsyn, K. Omura, S. Kimura, S. Yoshii, K. Okunishi, Z. He, T. Taniyama, M. Itoh, and M. Hagiwara. 'Novel Phase Transition Probed by Sound Velocity in Quasi-One-Dimensional Ising-Like Antiferromagnet $\text{BaCo}_2\text{V}_2\text{O}_8$.' *Journal of the Physical Society of Japan*, **80**, 033701 (2011). doi:10.1143/JPSJ.80.033701.
- ¹⁶¹ E. Canévet, B. Grenier, M. Klanjšek, C. Berthier, M. Horvatic, V. Simonet, and P. Lejay. 'Field-induced magnetic behavior in quasi-one-dimensional Ising-like antiferromagnet $\text{BaCo}_2\text{V}_2\text{O}_8$: A single-crystal neutron diffraction study.' *Phys. Rev. B*, **87**, 054408 (2013). doi:10.1103/PhysRevB.87.054408.
- ¹⁶² M. Enderle, C. Mukherjee, B. Fk, R. K. Kremer, J.-M. Broto, H. Rosner, S.-L. Drechsler, J. Richter, J. Malek, A. Prokofiev, W. Assmus, S. Pujol, J.-L. Raggazzoni, H. Rakoto, M. Rheinstädter, and H. M. Rønnow. 'Quantum helimagnetism of the frustrated spin- chain LiCuVO_4 .' *EPL (Europhysics Letters)*, **70**, 237 (2005).
- ¹⁶³ S. Nishimoto, S.-L. Drechsler, R. Kuzian, J. Richter, J. Mlek, M. Schmitt, J. van den Brink, and H. Rosner. 'The strength of frustration and quantum fluctuations in LiVCuO_4 .' *EPL (Europhysics Letters)*, **98**, 37007 (2012).
- ¹⁶⁴ F. Heidrich-Meisner, I. P. McCulloch, and A. K. Kolezhuk. 'Phase diagram of an anisotropic frustrated ferromagnetic spin- $\frac{1}{2}$ chain in a magnetic field: A density matrix renormalization group study.' *Phys. Rev. B*, **80**, 144417 (2009). doi:10.1103/PhysRevB.80.144417.
- ¹⁶⁵ A. Kolezhuk and T. Vekua. 'Field-induced chiral phase in isotropic frustrated spin chains.' *Phys. Rev. B*, **72**, 094424 (2005). doi:10.1103/PhysRevB.72.094424.
- ¹⁶⁶ T. Vekua, A. Honecker, H.-J. Mikeska, and F. Heidrich-Meisner. 'Correlation functions and excitation spectrum of the frustrated ferromagnetic spin- $\frac{1}{2}$ chain in an external magnetic field.' *Phys. Rev. B*, **76**, 174420 (2007). doi:10.1103/PhysRevB.76.174420.
- ¹⁶⁷ L. Svistov, T. Fujita, H. Yamaguchi, S. Kimura, K. Omura, A. Prokofiev, A. Smirnov, Z. Honda, and M. Hagiwara. 'New high magnetic field phase of the frustrated $S = 1/2$ chain compound LiCuVO_4 .' *JETP Letters*, **93**, 21–25 (2011). ISSN 0021-3640. doi:10.1134/S0021364011010073.
- ¹⁶⁸ N. Büttgen, H.-A. Krug von Nidda, L. E. Svistov, L. A. Prozorova, A. Prokofiev, and W. Assmus. 'Spin-modulated quasi-one-dimensional antiferromagnet LiCuVO_4 .' *Phys. Rev. B*, **76**, 014440 (2007). doi:10.1103/PhysRevB.76.014440.
- ¹⁶⁹ N. Büttgen, W. Kraetschmer, L. E. Svistov, L. A. Prozorova, and A. Prokofiev. 'NMR study of the high-field magnetic phase of LiCuVO_4 .' *Phys. Rev. B*, **81**, 052403 (2010). doi:10.1103/PhysRevB.81.052403.
- ¹⁷⁰ N. Büttgen, P. Kuhns, A. Prokofiev, A. P. Reyes, and L. E. Svistov. 'High-field NMR of the quasi-one-dimensional antiferromagnet LiCuVO_4 .' *Phys. Rev. B*, **85**, 214421 (2012). doi:10.1103/PhysRevB.85.214421.
- ¹⁷¹ K. Nawa, M. Takigawa, M. Yoshida, and K. Yoshimura. 'Anisotropic Spin Fluctuations in the Quasi One-Dimensional Frustrated Magnet LiCuVO_4 .' *Journal of the Physical Society of Japan*, **82**, 094709 (2013). doi:10.1143/JPSJ.82.094709.
- ¹⁷² T. Masuda, M. Hagihara, Y. Kondoh, K. Kaneko, and N. Metoki. 'Spin Density Wave in Insulating Ferromagnetic Frustrated Chain LiCuVO_4 .' *Journal of the Physical Society of Japan*, **80**, 113705 (2011). doi:10.1143/JPSJ.80.113705.
- ¹⁷³ M. Mourigal, M. Enderle, B. Fåk, R. K. Kremer, J. M. Law, A. Schneidewind, A. Hiess, and A. Prokofiev. 'Evidence of a Bond-Nematic Phase in LiCuVO_4 .' *Phys. Rev. Lett.*, **109**, 027203 (2012). doi:10.1103/PhysRevLett.109.027203.
- ¹⁷⁴ M. Enderle, B. Fåk, H.-J. Mikeska, R. K. Kremer, A. Prokofiev, and W. Assmus. 'Two-Spinon and Four-Spinon Continuum in a Frustrated Ferromagnetic Spin-1/2 Chain.' *Phys. Rev. Lett.*, **104**, 237207 (2010). doi:10.1103/PhysRevLett.104.237207.
- ¹⁷⁵ M. Yamashita, T. Shibauchi, and Y. Matsuda. 'Thermal-Transport Studies on Two-Dimensional Quantum Spin Liquids.' *ChemPhysChem*, **13**, 74–78 (2012). ISSN 1439-7641. doi:10.1002/cphc.201100556.
- ¹⁷⁶ P. A. Lee, N. Nagaosa, and X.-G. Wen. 'Doping a Mott insulator: Physics of high-temperature superconductivity.' *Rev. Mod. Phys.*, **78**, 17–85 (2006). doi:10.1103/RevModPhys.78.17.
- ¹⁷⁷ S. Sachdev. 'Exotic phases and quantum phase transitions: model systems and experiments.' *ArXiv:0901.4103* (2009). 0901.4103.
- ¹⁷⁸ B. J. Powell and R. H. McKenzie. 'Quantum frustration in organic Mott insulators: from spin liquids to unconventional superconductors.' *Reports on Progress in Physics*, **74**, 056501 (2011).
- ¹⁷⁹ Z. Hiroi and M. Ogata. 'Metallic and Superconducting Materials with Frustrated Lattices.' In C. Lacroix, P. Mendels, and F. Mila, editors, 'Introduction to Frustrated Magnetism,' volume 164 of *Springer Series in Solid-State Sciences*, pages 587–627. Springer Berlin Heidelberg (2011). ISBN 978-3-642-10588-3. doi:10.1007/978-3-642-10589-0.22.
- ¹⁸⁰ C. Hotta. 'Quantum electric dipoles in spin-liquid dimer Mott insulator $\kappa - (\text{bedt} - \text{ttf})_2\text{cu}_2(\text{cn})_3$.' *Phys. Rev. B*, **82**, 241104 (2010). doi:10.1103/PhysRevB.82.241104.
- ¹⁸¹ H. Kino and H. Fukuyama. 'Electronic States of Conducting Organic κ -(BEDT-TTF) $_2\text{X}$.' *Journal of the Physical Society of Japan*, **64**, 2726–2729 (1995). doi:10.1143/JPSJ.64.2726.
- ¹⁸² L. F. Tocchio, H. Feldner, F. Becca, R. Valentí, and C. Gros.

- ‘Spin-liquid versus spiral-order phases in the anisotropic triangular lattice.’ *Phys. Rev. B*, **87**, 035143 (2013). doi:10.1103/PhysRevB.87.035143.
- ¹⁸³ G. Misguich, B. Bernu, C. Lhuillier, and C. Waldtmann. ‘Spin Liquid in the Multiple-Spin Exchange Model on the Triangular Lattice: ^3He on Graphite.’ *Phys. Rev. Lett.*, **81**, 1098–1101 (1998). doi:10.1103/PhysRevLett.81.1098.
- ¹⁸⁴ O. I. Motrunich. ‘Variational study of triangular lattice spin-12 model with ring exchanges and spin liquid state in $\kappa\text{-(ET)}_2\text{Cu}_2(\text{CN})_3$.’ *Phys. Rev. B*, **72**, 045105 (2005). doi:10.1103/PhysRevB.72.045105.
- ¹⁸⁵ H.-Y. Yang, A. M. Läuchli, F. Mila, and K. P. Schmidt. ‘Effective Spin Model for the Spin-Liquid Phase of the Hubbard Model on the Triangular Lattice.’ *Phys. Rev. Lett.*, **105**, 267204 (2010). doi:10.1103/PhysRevLett.105.267204.
- ¹⁸⁶ C. Xu and S. Sachdev. ‘Global phase diagrams of frustrated quantum antiferromagnets in two dimensions: Doubled Chern-Simons theory.’ *Phys. Rev. B*, **79**, 064405 (2009). doi:10.1103/PhysRevB.79.064405.
- ¹⁸⁷ M. Barkeshli, H. Yao, and S. A. Kivelson. ‘Gapless spin liquids: Stability and possible experimental relevance.’ *Phys. Rev. B*, **87**, 140402 (2013). doi:10.1103/PhysRevB.87.140402.
- ¹⁸⁸ D. N. Sheng, O. I. Motrunich, and M. P. A. Fisher. ‘Spin Bose-metal phase in a spin- $\frac{1}{2}$ model with ring exchange on a two-leg triangular strip.’ *Phys. Rev. B*, **79**, 205112 (2009). doi:10.1103/PhysRevB.79.205112.
- ¹⁸⁹ R. V. Mishmash, J. R. Garrison, S. Bieri, and C. Xu. ‘Theory of a Competitive Spin Liquid State for Weak Mott Insulators on the Triangular Lattice.’ *Phys. Rev. Lett.*, **111**, 157203 (2013). doi:10.1103/PhysRevLett.111.157203.
- ¹⁹⁰ M. Abdel-Jawad, I. Terasaki, T. Sasaki, N. Yoneyama, N. Kobayashi, Y. Uesu, and C. Hotta. ‘Anomalous dielectric response in the dimer Mott insulator $\kappa\text{-(BEDT-TTF)}_2\text{Cu}_2(\text{CN})_3$.’ *Phys. Rev. B*, **82**, 125119 (2010). doi:10.1103/PhysRevB.82.125119.
- ¹⁹¹ R. S. Manna, M. de Souza, A. Brühl, J. A. Schlueter, and M. Lang. ‘Lattice Effects and Entropy Release at the Low-Temperature Phase Transition in the Spin-Liquid Candidate $\kappa\text{-(BEDT-TTF)}_2\text{Cu}_2(\text{CN})_3$.’ *Phys. Rev. Lett.*, **104**, 016403 (2010). doi:10.1103/PhysRevLett.104.016403.
- ¹⁹² M. Naka and S. Ishihara. ‘Electronic Ferroelectricity in a Dimer Mott Insulator.’ *Journal of the Physical Society of Japan*, **79**, 063707 (2010). doi:10.1143/JPSJ.79.063707.
- ¹⁹³ N. Gomes, R. T. Clay, and S. Mazumdar. ‘Absence of superconductivity and valence bond order in the HubbardHeisenberg model for organic charge-transfer solids.’ *Journal of Physics: Condensed Matter*, **25**, 385603 (2013).
- ¹⁹⁴ H. Seo, C. Hotta, and H. Fukuyama. ‘Toward Systematic Understanding of Diversity of Electronic Properties in Low-Dimensional Molecular Solids.’ *Chemical Reviews*, **104**, 5005–5036 (2004). doi:10.1021/cr030646k. PMID: 15535640, <http://pubs.acs.org/doi/pdf/10.1021/cr030646k>.